The Pennsylvania State University

The Graduate School

The Department of Energy and Mineral Engineering

AUTOIGNITION OF N-HEPTANE, ETHANOL, METHYL HEXANOATE AND METHYL 3-HEXENOATE IN A MOTORED ENGINE

A Thesis in

Energy and Mineral Engineering

by

Orin D. Moyer

Submitted in Partial Fulfillment
of the Requirements
for the Degree of

Master of Science

December 2011

The thesis of Orin D. Moyer was reviewed and approved* by the following:

André L. Boehman
Professor of Fuel Science and Materials Science and Engineering
Thesis Advisor

Semih Eser
Professor of Energy and Geo-Environmental Engineering

Robert L. Grayson
Professor of Energy and Mineral Engineering

*Signatures are on file in the Graduate School

ABSTRACT

Autoignition of fuel blends consisting of ethanol, n-heptane, and two biodiesel surrogates: methyl hexanoate (mhx) and methyl 3-hexenoate (m3h) were studied in a Cooperative Fuels Research (CFR) motored-engine at equivalence ratios (Φ) 0.25 and 0.50 (typical Φ of HCCI and diesel engine operation) with an intake temperature of 155ºC. The objectives of the study were to further understand the low-temperature oxidation chemistry of the four pure fuels and their blends, to compare the effect of a saturated and unsaturated methyl ester containing the same number of carbon atoms as n-heptane, to observe the intermediate species by GS-MS and GC-FID examination of exhaust samples taken prior to the autoignition event, and to study the impact of ethanol on each of the methyl esters . The compression ratio of the CFR engine was gradually increased from the lowest point to the point where the onset of high-temperature heat-release (HTHR) occurred. Within the test range of this research, all fuels and their blends where driven to their critical compression ratio (the onset of HTHR); and it was observed through heat-release analysis and of CO emissions trends comparison that the saturated methyl ester (mhx) exhibited cool-flame behavior while its unsaturated counterpart did not. This observation agrees with previous studies by Zhang and Boehman that the presence of a double-bond in the aliphatic chain suppresses cool-flame behavior by inhibiting isomerization reactions of peroxy radicals that are key to low-temperature oxidation chemistry. All blends with ethanol had a roughly linear effect on the delay of the onset of HTHR. Another trend observed was that blends with increasing ethanol content had a lower magnitude of LTHR and an onset occurring further after top dead center at the same compression ratio indicating that blends with increasing ethanol content are less reactive in the low-temperature regime. Interestingly, the magnitude of LTHR increases with increasing compression ratio for mhx/hept blends while the magnitude of LTHR was noted to decrease for pure mhx. Further, it was observed that the magnitude of the LTHR *at the critical compression ratio* decreases with increasing ethanol content for pure mhx and its n-heptane blends as a result of the inhibiting effect of ethanol on ignition.

TABLE OF CONTENTS

LIST OF FIGURES

LIST OF TABLES

LIST OF ACRONYMS

AHHR: apparent heat-release rate
ASTM: American Society for Testing and Materials
BFEC: brake specific energy consumption
BMEP: brake mean effective pressure
BSFC: brake specific fuel consumption
CA: crank angle
CFR: cooperative fuel research
CO: carbon monoxide
CO_2: carbon dioxide
CR: compression ratio
cSt: centistokes
DOC: diesel oxidation catalyst
DPF: diesel particulate filter
EBD: ethanol-biodiesel-diesel
EBSFC: equivalent brake specific fuel consumption
EGR: exhaust gas recirculation
FAAEs: fatty acid alkyl esters
FAMEs: fatty acid methyl esters
FT: Fischer–Tropsch
GCFID: gas chromatography-flame ionization detector
GCMS: gas chromatography-mass spectrometry
HCCI: homogeneous charge compression ignition
HTHR: high-temperature heat-release
LNTs: lean NO_x traps
LTHR: low-temperature heat-release
m3h: methyl 3-hexenoate
mhx: methyl hexanoate
NO_x: nitrogen oxides
NTC: negative temperature coefficient
PM: particulate matter
ppm: parts per million
RME: rapeseed methyl ester
SCR: selective catalytic reduction
SOF: soluble organic fraction
TDC: top dead center
THC: total hydrocarbons
VOC: volatile organic compound
Φ: equivalence ratio

ACKNOWLEDGEMENTS

I would first like to thank my thesis advisor Professor André Boehman for his support and encouragement throughout my graduate career at Penn State. It was an honor to have the opportunity to be part of his research group and study in the engine lab at the Energy Institute. I am especially thankful for his guidance on the selection of my thesis topic and his continued resourcefulness in finding funding for fuels and other miscellaneous research items that have helped me succeed.

I would also like to thank visiting Professor John Agudelo of Columbia for his patience and skillful mentoring in conducting the experiments on the CFR engine and collecting exhaust gas samples. I am also appreciative of his guidance with the data analysis. In addition, I would like to thank visiting Professor Magin Lapuerta of Spain for his support and guidance.

Many thanks go out to my fellow graduate students at Penn State for their assistance and guidance throughout the graduate program. Particular thanks go out to Greg Lilik for his skillful and specialized preparation of the CFR engine, AVL bench, and coding of the Labview data acquisition software.

Chapter 1
Introduction

The rising trends of energy consumption and fossil fuel depletion are intensifying; and other challenging problems such as emissions control are increasingly difficult. Such issues have pushed the incorporation of renewable energy fuels, higher efficiency engines, and state of the art emission control technologies. Advanced exhaust gas aftertreatment to reduce soot and NO_x emissions using regenerative traps and catalytic reduction are already being implemented. Expanding the use of renewable energy sources such as ethanol and biodiesel requires advances in production, cost reduction, and in some cases consideration of environmental impact. Bio-ethanol can be produced from a number of crops including sugarcane, corn, wheat, and sugar beet through fermentation. Biodiesel can be produced from straight vegetable oil, edible and non-edible, recycled waste vegetable oils, and animal fats economically via the transesterification process. There are several factors that do need to be considered before recommending the usage of alternative fuels such as ethanol and biodiesel. Such considerations may include the extent of modifications required to existing engines and investment costs of processing, transportation, and distribution infrastructure[1].

Recent interest has been towards blending ethanol and biodiesel with petroleum diesel in order to incorporate a renewable fuel content. Renewable content is desirable in order to reduce the consumption rate of Earth's limited petroleum fuels. In addition, when biodiesel and ethanol are blended with petroleum diesel they have the ability to improve emissions properties and engine performance [1-6], which will be discussed in more detail throughout this paper. Ethanol, of course, is not a good diesel fuel by itself. It has an unacceptably low cetane number, lower viscosity than conventional petroleum diesel and biodiesel, lower lubricity, reduced ignitability as well as other complications[2]. The high viscosity of unaltered vegetable oil, 35–60 centistokes (cSt) compared to 4 cSt for diesel, leads to problems in pumping and spray characteristics and is not feasible to run in a diesel engine[1, 7]. Also, the inefficient mixing of high viscosity oil with air contributes to incomplete combustion. This results in high carbon deposit formation, injector coking, piston ring sticking, and lubricating oil dilution and degradation. Because of these

problems, vegetable oils must be chemically modified to a more suitable and compatible fuel for existing engines.

The solution is to trans-esterify the oils with short-chain aliphatic alcohols (typically methanol) in order to form fatty acid alkyl esters (FAAEs) which can bring their combustion-related properties closer to those of mineral diesel. Transesterification is the exchanging of the alkoxy group of an ester compound by an alcohol, (Equation 1). An example is the reaction of a triglyceride (fats and oils) with methanol to form a methyl ester biodiesel. Typical conditions when using methanol are a molar ratio of alcohol to vegetable oil of 6:1 at 60–65ºC for 1 hour at ambient pressure[3]. These reactions can be catalyzed with an acid or base catalyst. Currently, base-catalyzed (sodium or potassium hydroxide) transesterification is the most efficient and economic process. Since the reaction is reversible, excess alcohol is required to shift the equilibrium to the product side[1].

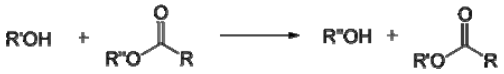

Equation 1. Transesterification

The result is biodiesel, which is defined as alkyl esters of vegetable oils or animal fats. The fatty acid profile of biodiesel corresponds to the parent oil or fat from which it is obtained[3]. The major components of biodiesel fuels are straight-chain fatty acids. The most common ones contain 16 or 18 carbon atoms. In any case, biodiesel is capable of being run directly in current diesel engines or blended at any ratio with conventional diesel with little or no engine modifications, but suffers notably from increased NO_x emissions due to increased cylinder temperature and pressure (which increase the rate of NOx formation) caused by complex shifts in flame stoichiometry and localized temperature as described by the works of Mueller et al.[8] Also worth noting is that due to its lower heating value, biodiesel will produce less torque in an unmodified diesel engine, as depicted in Figure 1. It is likely, however, that torque can be increased by increasing fuel flow rates.

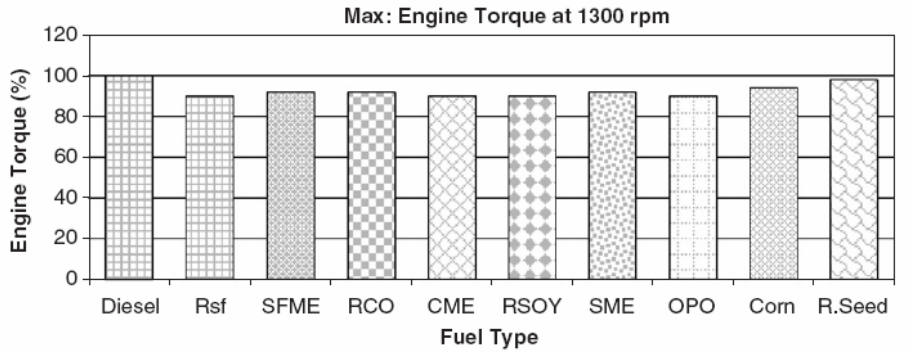

Figure 1. Effect of biodiesel fuel type on engine torque [1]

Both biodiesel and ethanol share an interesting ingredient of fuel-bound oxygen. There are many effects of this fuel-bound oxygen component, ranging from beneficially completing the combustion process to complicating diesel engine injection timings. It has been observed that advances in fuel injection timing may be related to differences in the bulk modulus between different fuels[9]. Szybist and Boehman[10], for example, concluded that increasing biodiesel concentration caused the fuel injection to advance in a nearly linear manner. Injection timing is often overlooked when authors compare emissions of similar fuels in different engines, but it can have a significant effect, especially on NOx and PM due to changes in the cylinder pressure and volume. Retarded injection timings may lead to lower NOx and PM emissions because of lower cylinder temperatures.

In addition to biofuels, metal-based additives can be used to decrease emissions through such mechanisms as reacting with water to produce hydroxyl radicals (which enhance soot oxidation) or by reacting directly with carbon atoms in the soot, thereby lowering the oxidation temperature[11]. The scope of this paper, however, will not include discussion of metals as additives to diesel fuels.

Chapter 2
Literature Review

2.1 Diesel Engines

Diesel engines are capable of delivering higher fuel economy than gasoline engines but tend to suffer from increased Nitrogen Oxide (NO_x) emissions. A fundamental understanding of how diesel fuels and their blends effect compression ignition engines is important for achieving optimal performance, especially when incorporating ethanol and biodiesel blends. Due to the inherent nature of the diesel combustion process there is a tradeoff between NO_x emissions and PM emissions[12]; thus, it is difficult to have a simultaneous reduction of both. Some of the emissions can be decreased by blending ethanol and biodiesel with conventional diesel. Current strategies are generally aimed at the reduction of one of the two emissions during the combustion process and the other in an aftertreatment device. It is understood that NO_x emissions tend to increase with higher temperatures and that PM emissions can be decreased by higher temperatures due to a more complete combustion process. There are other factors that contribute to emissions such as injection timing and composition of the fuels. When talking about a diesel engine, arguably the most important consideration of the combustion characteristic is the cetane number. Cetane number is a function of the composition and the structure of the hydrocarbons present in the diesel. It tends to decrease with an increase in aromatic hydrocarbon content and increases with an increase of n-paraffin and olefin content.

Improved ignition of high cetane fuels are detected as a decrease in the ignition delay time, where the ignition delay time is measured as the time between the start of fuel injection and detectable ignition (high-temperature heat-release, HTHR). Shorter ignition delay times have been directly correlated with a faster startup in cold weather, reduced NOx emissions, and smoother engine operation[11]. In some cases, diesel ignition improvers may be added to the fuel blend. Ignition improvers are species such as ethyl-hexyl nitrate that decompose at lower temperatures than the ignition temperature provided by H_2O_2 decomposition. Radicals produced

by decomposition of the additive consume some fuel and release heat, raising the temperature of the premixed gases and getting them closer to the H_2O_2 decomposition temperature[13]. Other additives that decompose at lower temperatures and provide radicals could also be effective diesel ignition improvers or cetane improvers.

2.2 Properties of Ethanol-Biodiesel-Diesel Blends

2.2.1 Oxygen Content

With the use of ethanol and biodiesel comes fuel-born oxygen. Combustion studies have shown that fuel-born oxygen aids in completing the combustion process by ensuring oxygen is available to otherwise fuel rich regions[4]. This entrainment is thought to improve the combustion process in many ways. First, the improved mixture allows an increased possibility for complete diesel combustion due to extra oxygen availability. Where oxygen is limited, incomplete combustion will dominate; and less fuel burnt means less useful power as well as increased emissions of unburned hydrocarbons and carbon monoxide[14]. Fuel-born oxygen has also been attributed to a reduction in the formation and growth of soot nuclei; and studies have shown that when fuel-born oxygen content is in excess of 30% (wt basis) that combustion is almost smokeless[15]. Also of interest in the oxidation behavior of fuels is the functional group origin of the oxygen. The differences between ethanol and biodiesel as they relate to combustion will be discussed throughout this paper. In biodiesel the oxygen belongs to the ester group while the oxygen component of ethanol belongs to the hydroxyl group. Other compounds can be added to increase the oxygen content of a fuel such as ethers, acetates and carbonates; however, the focus of this work is on ethanol (alcohol) and biodiesel (alkyl esters).

2.2.2 Stability

Stability of ethanol-biodiesel diesel blends refers to the phase separation that occurs in a mixture under given conditions. For ethanol-diesel blends, as the temperature decreases or ethanol content increases, the mixture becomes less stable and the time it takes to separate into

different phases decreases[16-18]. Water presence in e-diesel blends also favors separation of the ethanol phase; as water content increases, the separation occurs at even lower initial ethanol content, narrowing the stability zone[16]. There are two main strategies aimed at improving the stability of e-diesel blends. The first is through the usage of surfactants (emulsifiers) that produce stable emulsions and the second is addition of cosolvents that produce stable solutions. Surfactants are compounds that lower the surface tension of a liquid - the interfacial tensions between two liquids. Cosolvents might be considered easier to prepare, as they can be prepared with simple splash blending. Preparing e-diesel blends using emulsifiers tends to be more complicated, as preparation requires a heating and a stirring step[11].

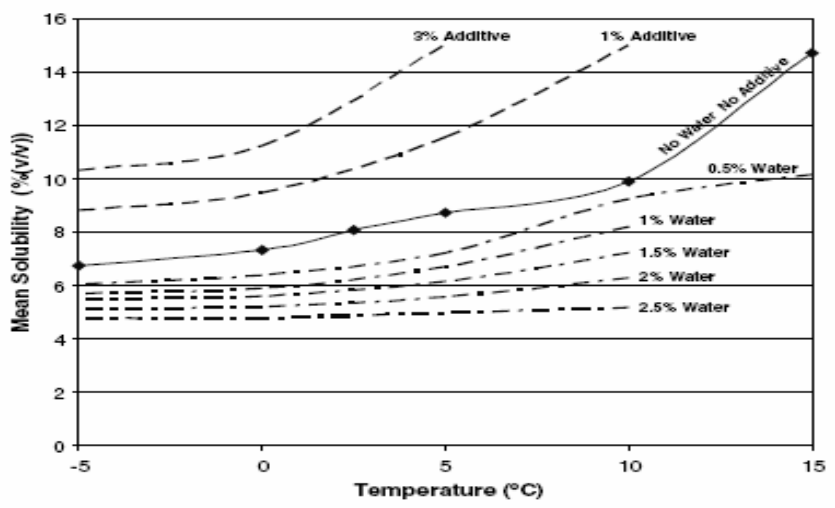

Figure 2. Effect of water and additive on mean solubility [16]

We can see from Figure 2 that an additive is required if blends of ethanol greater than 7% are to remain stable below 0ºC. The additive was O_2Diesel in this study[16]. In the presence of water, the solubility of ethanol with diesel is further depressed[11]. Even as small an amount of water as 1% can make e-diesel blends of 5% unstable below 0ºC. This is explained by the higher polarity of water as compared to ethanol and its preferential dipole interaction with the polar components of diesel[11]. It can also be seen that the sensitivity of the blend increases as temperature increases, especially at 10ºC for blends with no water or additive (the solid line in Figure 2). Practical limits for stability additives are about 2%, thus we can observe from Figure 2 that blends of 10% ethanol (on a volume basis) with 2% O_2Diesel additive can be used in regions where temperatures rarely fall below -5ºC [16]. Conveniently, biodiesel acts as a stabilizer in e-diesel blends[18-20] and is a positive reason for ethanol-biodiesel-diesel (EBD) blending. Figure 3

shows the blending stability of ethanol and higher alcohols with diesel fuel. The unstable zones reside below each curve. Figure 3 is, in essence, an extension of Figure 2; and the practical upper limit of ethanol blending (orange curve in Figure 3) without additives is seen to be about 10%, at which point the slope increases exponentially. Also noticeable from Figure 3 is that higher alcohols consisting of three or more carbon atoms (such as propanol and butanol) have a much wider stability zone than ethanol due to their lower polarity[17]. As a reference to the reader, diesel fuels containing higher n-paraffin content are generally less polar than those containing higher aromatic contents[11]. Thus, we can infer that diesel fuels with higher aromatic content (although detrimental to the cetane number) can be blended in higher concentrations of ethanol with regard to phase separation stability.

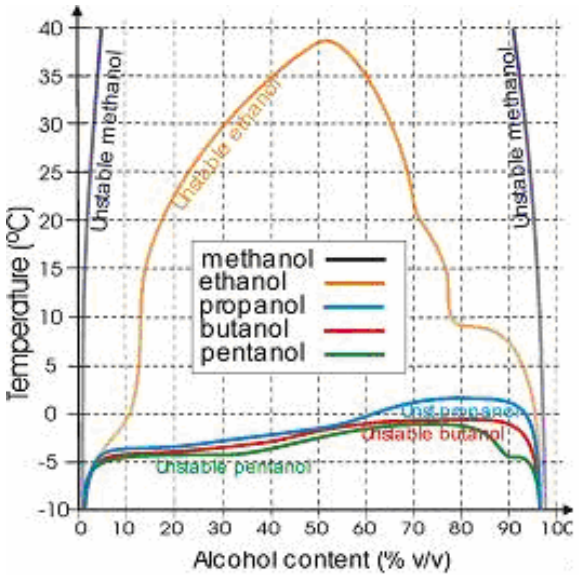

Figure 3. Blending stability of alcohols without additive in diesel fuel [17]

In addition to blending stability, another issue with biodiesel is its oxidation stability. Unsaturated fatty acid esters (such as methyl 3-hexenoate used in the current study) are unstable with respect to light, catalytic systems, and atmospheric oxygen[11]. Since this is not a problem with petrol diesel, automotive companies have not considered fuel degradation when designing diesel engines and vehicles. Oxidation can be visibly noted by the color change of biodiesel from yellow to brown, and causes a slight reduction in heating value and a large change in kinematic viscosity bringing it above levels stipulated by ASTM D6751 [21]. Creation of oxidation products before combustion can lead to solid materials and gums blocking fuel filters and injectors[21].

There are several mechanisms through which biodiesel can degrade. The main mechanism is auto-oxidation, where oxygen reacts with a biodiesel molecule via a radical mechanism and is accelerated by higher thermal conditions. Two other mechanisms are photo-oxidation in the presence of light and a reverse transesterification reaction that occurs under acidic conditions[21]. It is, however, possible to circumvent these issues with the use of additional additives, antioxidants, which inhibit oxidation.

2.2.3 Viscosity

Diesel quality limits are set to minimum of 2.0 centistokes (cSt) so it is important to understand the effects of ethanol on e-diesel blends. As a reference for the reader, the kinematic viscosity of water and diesel are approximately 1.0 cSt and 4.0 cSt, respectively. Experimental data from reference [17] have been reproduced in Figure 4 to show the effect of e-diesel blends of increasing ethanol content on viscosity. In fact, the data show that it is only possible to blend up to 20% ethanol (v/v) before ASTM viscosity requirements are no longer met.

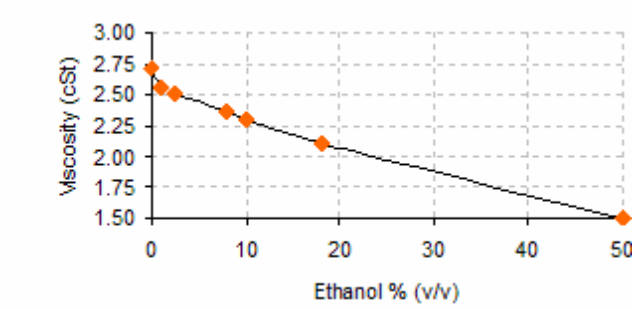

Figure 4. Effect of ethanol blending on viscosity (reproduced from Lapuerta et al. [17])

It was hypothesized by Lapuerta et al. that blending ethanol would compensate somewhat for the diesel fuel cold plugging point (CPP) in cold weather conditions[17]. It was discovered, however, that blends of very high alcohol percentages (>50%) would be necessary. Due to the many negative effects of e-diesel blends over 20%, it was concluded that ethanol could not be considered to have a positive effect on CPP [17]. While the similarities of biodiesel to petroleum diesel allow the use of any blend in a diesel engine, the poor cold flow characteristics of biodiesel is a barrier that must be considered in cold weather application.

2.2.4 Lubricity

Lubricity additives form boundary films between metal-to-metal surfaces preventing contact between metals that leads to engine wear[11]. In most low-sulfur diesel/biodiesel blends an additional lubricity additive is not required since the vegetable-oil methyl esters already enhance the fuel lubricity[11]. According to one review[11], fatty compounds have better lubricity than hydrocarbons because of their polarity-imparting oxygen atoms. The same review also suggests that fatty acid esters derived from vegetable oils can increase diesel lubricity at concentrations as low as 1%[11]. Turning attention from biodiesel to ethanol, although the lubricity of alcohols is worse than required by diesel specifications, blends with ethanol are better than expected as a consequence of alcohol evaporation from the lubricating layer[17, 20]. Studies have concluded that blending of ethanol even up to 20% (volume basis) still falls within acceptable wear scar limits[17]. A final note on lubricity is that ultra low sulfur petroleum diesels have poor anti-wear properties but anti-wear additives such as methyl esters (biodiesel) can be blended to significantly improve performance[11].

2.3 Engine Performance and Efficiency

A diesel engine (also known as a compression ignition engine) uses compression to initiate autoignition in order to burn fuel. Diesel engines work by injecting air into the combustion chamber which is subsequently compressed with a compression ratio typically between 15:1 and 22:1. The high compression heats the air to ~550ºC. Then, at about the top of the compression stroke, fuel is injected directly into the compressed air in the combustion chamber via a fuel injector which ensures the fuel is broken down into small droplets and distributed evenly. The heat of the compressed air vaporizes fuel from the surface of the droplets and the vapor eventually autoignites under the increased temperature and pressure. The rapid expansion of combustion gases drives the piston downward which supplies power to the crankshaft. Compared to gasoline engines, direct injection diesel engines are more fuel-efficient and capable of achieving higher torque due to increased compression ratios of diesel engines. Recent trends of adding biofuels to petroleum diesel blends in order to incorporate a renewable component have opened new opportunities due to the fuel oxygen content of biodiesel and

ethanol which have the ability to improve emission performances. In addition to emissions, the effects of oxygenated fuels on torque output, ignition properties, and brake specific fuel consumption are reviewed here. One example of an issue pertaining to ethanol-diesel blends greater than 30% is engine misfire occurring well after top dead center (TDC), especially at high engine speeds[15]. This is due to the ignition delay caused by the low cetane number of such e-diesel blends. Lastly, the alkyl chain length of esters as it pertains to ignition delay will be reviewed.

2.3.1 Engine Performance

Engine power is directly proportional to torque. This makes torque a good method of quantifying engine output. Studies have shown that the torque decreases throughout the entire speed at full load of an unmodified diesel engine when using oxygenated blends, as shown in Figure 5 (a)[15]. We can see from Figure 5 (b) that torque is reduced with increasing oxygen content by a relatively linear correlation.

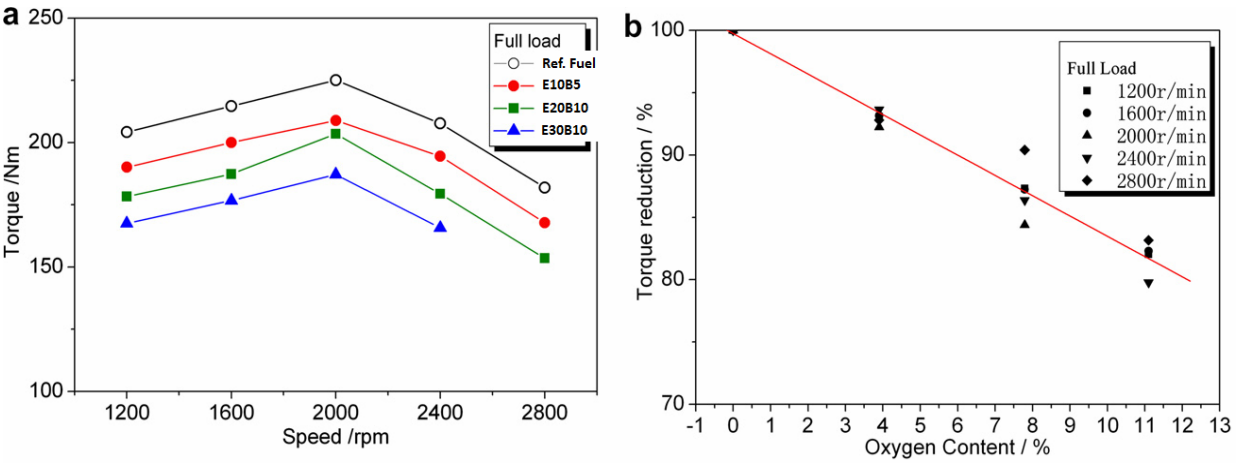

(a) (b)

Figure 5. Effect of oxygen content on torque [15]

The main reason for decreasing torque is the decreased heating value of ethanol and biodiesel - with respective heating values 35% and 12% less than reference diesel fuel (wt basis). The calculated power was 4% torque reduction for every 10% addition of ethanol[15]. Lower heating value is not the only factor responsible for power reduction. It was explained that the lower cetane value of the ethanol blends affects the combustion process[15]. Also, reduced

viscosity of the ethanol blends lead to reduction of the maximum fuel delivery capability, hence, reducing power output[5]. These tests were conducted in an unmodified engine, and it was suggested that certain modifications could improve performance. For example, the fueling capacity of the fuel injection system could be increased to improve power output. In addition, the compression ratio and fuel injection timing should be optimized for ethanol-biodiesel-diesel (EBD) blends[15].

Detailed kinetic mechanisms for ester combustion are important in understanding the autoignition properties biodiesel components in diesel engines. The autoignition properties of linear methyl esters was studied in a rapid-compression machine by HadjAli et al.[22] and the results displayed in Figure 6. These results show that the ignition timing is quite different for a series of methyl esters ranging from methyl butanoate to methyl heptanoate. Methyl butanoate was the most resistant of the tested fuels to autoigniton[22]. This is consistent with the works of Gail et. al.[23], Szybist et. al.[24], and Zhang et. al.[25]. It is discussed that the reactivity increases with the length of the aliphatic chain. Their detailed analysis of the cool-flame region emphasized the importance of H-atom transfer reactions which are dependant on the fuel structure. Reactions that may form a six-membered ring transition state were found to be kinetically favored[22].

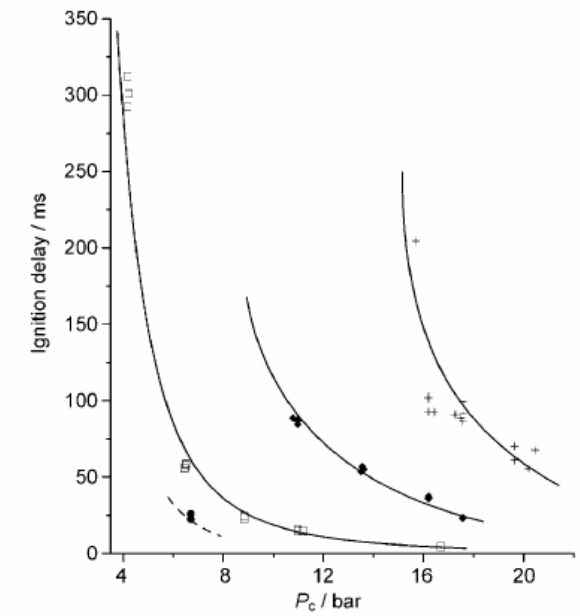

Figure 6. Autoignition delay times of fatty acid methyl esters at 815 K, at high pressures, studied in a rapid compression machine. Gas mixtures are stoichiometric with "air" (nitrogen is replaced by argon). Methyl butanoate (+), methyl pentanoate (◆), methyl hexanoate (□), and methyl heptanoate (●) [22]

2.3.2 Engine Efficiency

Fuel efficiency is measured in brake specific fuel consumption (BSFC). It is the amount of fuel an engine needs to consume in order to achieve a certain power output, typically measured in g/kWh - with lower values correspond to higher fuel efficiency. Fuels with increased oxygen content suffer from worsened BSFC due to lower heating values as mentioned previously. An interesting note, while biodiesel does have approximately 10% less energy density than conventional diesel on a weight basis, it has a higher specific gravity than diesel, 0.88 vs. 0.85. The overall impact is only about 5% lower energy content on a volume basis [1]. Because the power output of an engine has a correlation to energy density of the fuel, engines fueled with ethanol and biodiesel must consume more fuel to achieve the same power as conventional diesel.

Perhaps considered more useful in comparing different fuels is the equivalent brake specific fuel consumption (EBSFC) - also synonymous with brake specific energy consumption (BSEC). EBSFC is essentially a measure of the thermodynamic efficiency of the fuel. Figure 7 (a) shows that ethanol and biodiesel have different effects on BSFC. The general trend at higher engine speeds or increasing oxygen content is an increase in fuel consumption. The chart in Figure 7 (b) shows the EBSFC. It can be seen that the energy efficiencies of the four EBD fuels tested are actually very similar at the tested speeds.

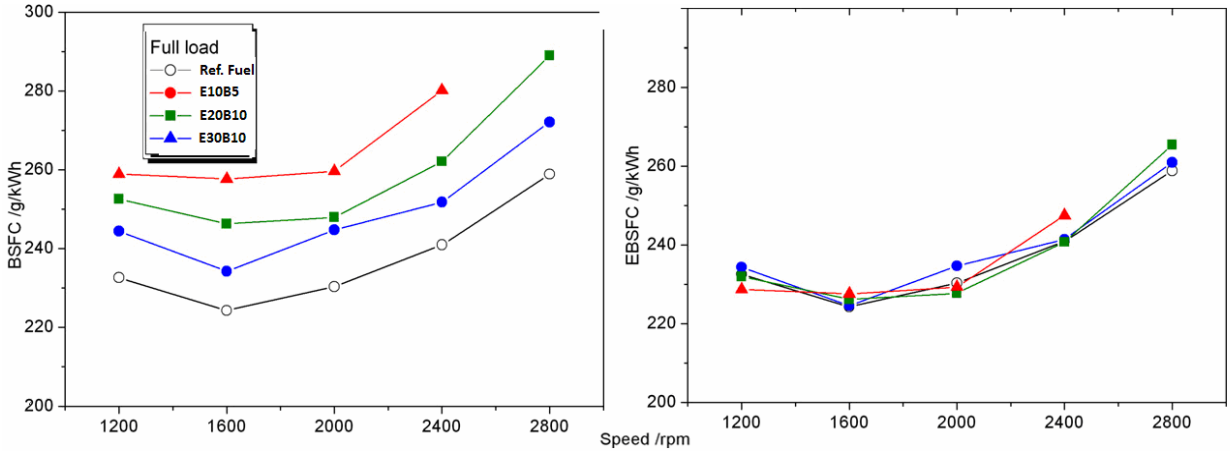

Figure 7. Brake specific fuel consumption of diesel and oxygenated blends [15]

Also of interest is the BSFC of ethanol-diesel blends without biodiesel. It was shown that ethanol-diesel blends up to 20% ethanol can be used in current compression ignition engines without any modification[1, 26]. As shown in Figure 8 the BSFC is increased when higher blending percentages of ethanol are used. These tests also showed that there was no significant reduction in power but thermal efficiency of ethanol blends of 15% and 20% suffered at medium and especially higher loads and can be seen in Figure 8 [1, 26].

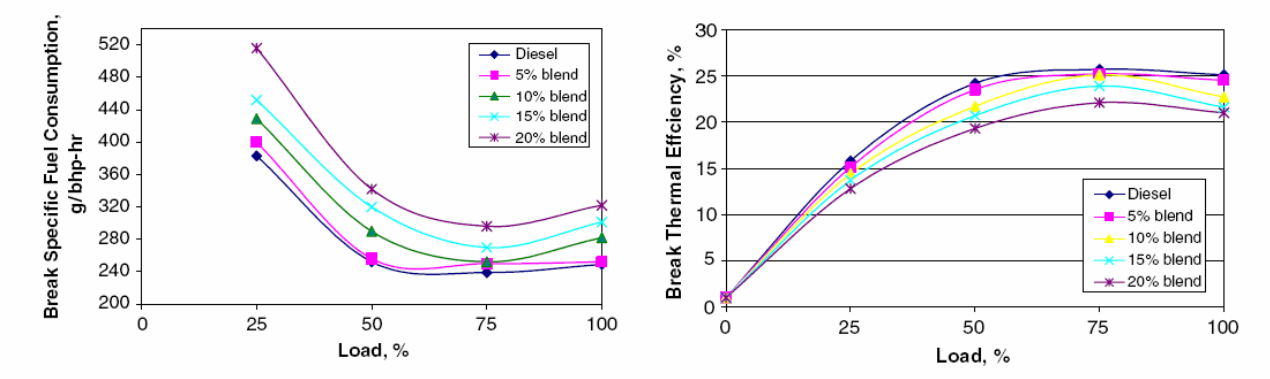

Figure 8. BSFC and BTE for ethanol diesel blends [26]

2.4 Emissions

2.4.1 Particulate Matter

Particulate matter (PM) from a diesel engine can be divided into soluble and insoluble fractions. The insoluble PM fraction is formed in the diffusion combustion process through pyrolytic heating of fuel-rich regions in the combustion chamber and is predominantly comprised of elemental carbon. This fraction is mostly consumed in the diffusion flame with the remaining portion agglomerating to form insoluble soot. The soluble portion of PM emissions are hydrocarbon species which condense and adsorb onto the insoluble particulate matter and further aid in the agglomeration process. Particulate matter contributions from individual components (paraffins, olefins, and aromatics) have been studied by other researchers and it was found that aromatics as a group are the greatest contributors [12]. Some researchers have shown that 80% of PM emissions are comprised of the insoluble fraction and that 20% belong to the soluble particulate fraction[12], however this can vary dramatically with engine, fuel, and operating conditions. With regard to particulate emissions, it has been suggested that fuel-compatible

oxygen-bearing compounds should be blended with diesel to produce a composite fuel containing between 10-25% volume of oxygenate [11].

Smaller particles remain suspended longer in aerosols, have larger specific surface areas which enables more hazardous substances to be adsorbed, are more difficult to retain in filters, and penetrate easier into respiratory systems - and to some extend, into the circulatory system. Because the size PM particles is directly linked to their potential for causing health problems, the EPA is concerned about particles that are 10 micrometers in diameter or smaller. Some studies have found that e-diesel blends are associated with a decrease in the mean particle diameter, and should be considered, in principle, a drawback[2]. It was concluded that the smaller size of the E10 blend tested was not caused by an increase in the smallest particles, but rather, a significant decrease in the largest particles; and that the apparent drawback may not have been as significant as initially claimed [2].

Smoke opacity is indicative of dry soot emissions, which are the main component of PM. Smoke opacity decreases as the ethanol content in the blends increases and the effect is further enhanced at high load[18]. One study examined the effect of smoke and PM on EBD blends of E10B5, E20B10, and E30B10 tested against a reference fuel. Figure 9 shows the PM (a) and smoke emissions (b) from an engine tested at increasing load.

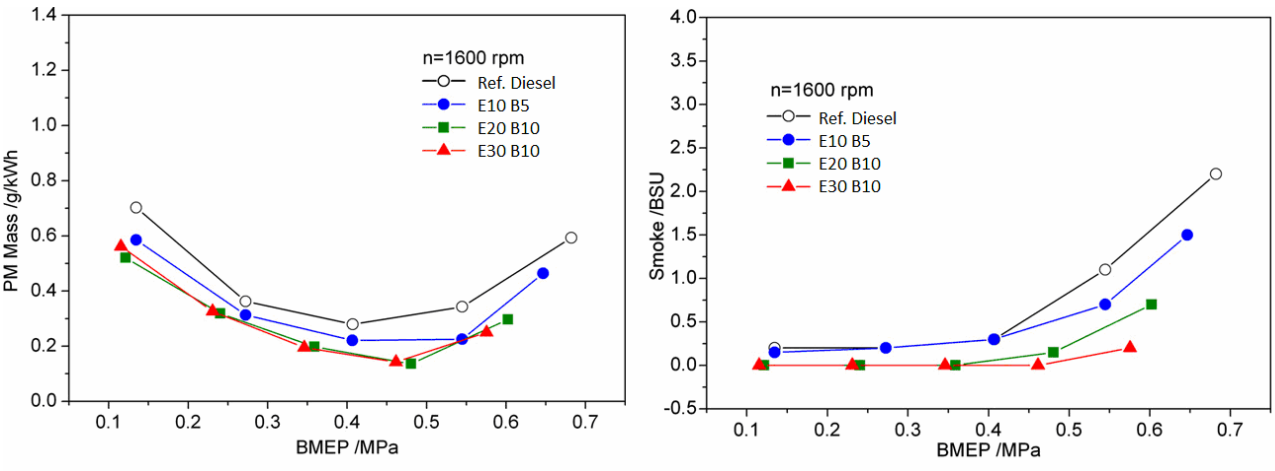

(a) **(b)**

Figure 9. Effect of oxygenated blends on PM and smoke [15]

Figure 9 (a) shows that all of the fuels tested emitted more PM at low and high loads and performed best at medium load. It is also shown that the addition of oxygenated blends reduced the PM by 25% to 50% until ethanol content reaches ~20% wt [15]. Figure 9 (b) shows that combustion is smokeless at low loads when 20% or more ethanol is blended. EBD blends (the red line in Figure 9) are shown to significantly reduce smoke at higher loads, and by as much as 85% reduction when employing E30B10 [15]. The lower opacity was explained due to the presence of fuel oxygen which reduces the probability of rich-zone formation (higher local fuel/air ratio) and promotes the oxidation of soot nuclei generated in fuel pyrolysis in the spray flame.

2.4.2 Nitrogen Oxides

NO_x is the generic term for NO and NO_2 (nitric oxide and nitrogen dioxide). The kinetics of NO_x formation are governed by the Zeldovich mechanism and its formation is highly dependent on temperature and the availability of oxygen [1]. The higher the gas temperature, the higher the rate of formation of NO_x [12]. NO_x typically consists of a mixture of 95% NO and 5% NO_2, corresponding to several hundred to several thousands parts per million for NO and tens parts per million (ppm) for NO_2 [27]. The main sources of NO_x emissions in combustion are the oxidation of molecular nitrogen in the post flame zone (thermal NO_x), formation of NO_x in the flame zone (prompt NO_x), and oxidation of nitrogen-containing organic compounds in the fuel (fuel NO_x) [27, 28]. The relative importance of these sources is dependent on the operating conditions and fuel type. For adiabatic combustion with excess oxygen, thermal NO_x formation is the predominant source of NO_x emissions [27]. NO_x emissions in actual systems have been observed to be highly dependent on excess air, which corresponds to lean running conditions [27]. The explanation for this is two-fold; first, a lean mixture will contain more oxygen to react; second, lean conditions (increased oxygen content) will typically burn hotter than a rich mixture which will increase the rate of NO_x formation. Based on the previous statements, one straightforward approach to reducing NO_x emissions is to avoid excessively high-temperatures and to reduce excess oxygen.

NO_x itself is a very weak greenhouse gas and should not be confused with nitrous oxide (N_2O), which is a very powerful greenhouse gas. The issues with NO_x are contributions to nitric

acid and its reaction with volatile organic compounds (VOCs) in the presence of sunlight to form photochemical smog which is a significant form of air pollution. NO_x will eventually convert to nitric acid in the presence of atmospheric moisture and become a significant component of acid rain. Nitrogen oxides react with water via reaction (a) to form nitrous oxide and nitric oxide. Nitrous oxides further decomposes into nitric acid via reaction (b).

(a) $2\ NO_2 + H_2O \rightarrow HNO_2 + HNO_3$

(b) $3\ HNO_2 \rightarrow HNO_3 + 2\ NO + H_2O$

Catalytic NO_x reduction technologies are attractive because of their relatively low cost and high efficiency. In principle, NO_x decomposition is thermodynamically favored at low-temperature. This reaction is very slow; however, and sufficiently effective ambient temperature catalysts have not been discovered thus far [28].

It can be seen from Figure 10 that increases in biodiesel content lead to increases in exhaust temperature at higher operation pressures and engine load. It is apparent that the increase in temperature along with the additional oxygen content belonging to the fuel will lead to higher quantity of NO_x in biodiesel-fueled engines.

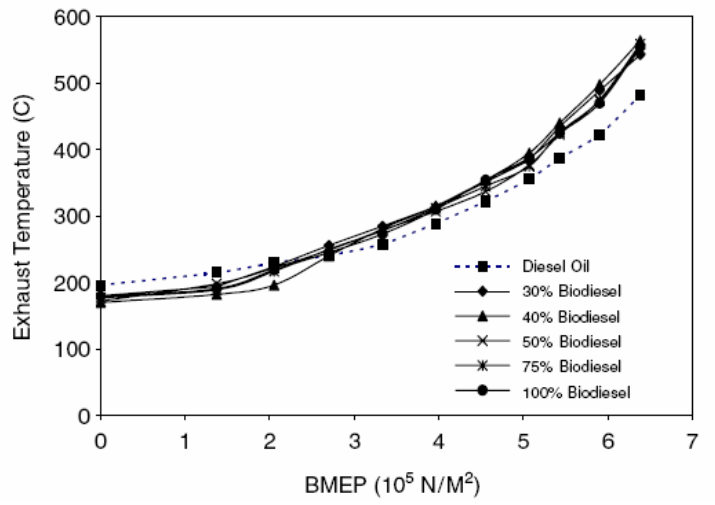

Figure 10. Effect of biodiesel content on exhaust temperature [1]

2.4.3 Carbon Monoxide

Oxygenated fuels, due to their inherent nature of a more complete combustion process[1], have the potential to significantly reduce carbon monoxide, which is formed by the incomplete

combustion of fuels. There appear to be several factors that impact the CO emissions of biodiesel. The primary reasons given by authors reporting CO increases include higher viscosity and poor spray characteristics for biodiesel, which lead to poor mixing and combustion [6]. Researchers reporting lower CO emissions often attribute the cause to the increased oxygen content and cetane number of biodiesel. Higher cetane number results in lower possibility of fuel rich zones, and thus reduces CO emissions. Advance in injection timing can have an effect on CO emissions, with general trends showing CO decreases when optimal injection strategies are employed[6]. The feedstock origin of the biodiesel also plays some part in determining CO emissions; and a general trend was found that methyl esters emitted less CO than ethyl esters and that increasing the aliphatic chain length corresponded with decreased CO emissions[6, 29]. Also to consider for CO emissions is addition of ethanol into biodiesel-diesel blends. The general trend among researchers is a reduction in CO emissions of EBD blends, especially at high loads[6, 29].

2.4.4 Total Hydrocarbons

Total hydrocarbons (THC) are a class of partially burned or unburned fuel emissions. Oxygenated fuel blends have different effect on THC emissions depending on the source of the oxygen functional group. In addition, THC emissions are not necessarily linearly correlated to oxygen content, thus the results must be verified experimentally. Such considerations to take into account for hydrocarbon emissions are the biodiesel blend percentage, feedstock, engine conditions, and alcohol additive. An extensive review paper by Xue, Grift, and Hansen [6] noted researchers who have actually reported increases in THC emissions from biodiesel, attributing the increase to poor atomization and lower volatility. However, only about 5% of studies reviewed here observe this increase[6]. A general trend appears to exist (~90% of papers reviewed) that neat biodiesel and biodiesel blends serve to reduce hydrocarbon emissions[6]. Although some researchers reported that THC emissions reductions were linear with increasing biodiesel content, others reported non-linear trends[6]. Also worth noting is that studies using e-diesel blends show an increase in unburned hydrocarbons[11], the opposite affect of biodiesel. This alludes to the fact that oxygen supplied by different functional groups has a different affect on HC emissions.

The oxygen content, cetane number, chain length, and saturation nature of biodiesel differs depending on the feedstock. Oxygen content contributes to more complete combustion and cetane number reduces burning delay; both result in reduced THC emissions. One study, for example, reported a typical methyl ester (in neat biodiesel form) reduced THC emissions by 45-67% [30]. A report by the National Renewable Energy Laboratory suggested that increasing chain length and saturation both attribute to decreases in THC emissions of neat biodiesel as compared to conventional diesel [31]. Engine operating conditions such as load and speed can also influence THC emissions, but the literature reports inconsistent results. A general trend appears to be decreases in THC at low load with the greatest decrease at medium load [6, 32]. As a note to the reader, none of the literature reviewed indicated an increase in THC emissions for biodiesel compared to conventional diesel as a result of load, only different degrees of reductions.

Ethanol percentage in a biodiesel-diesel blend also has an effect on THC emissions. Ethanol serves to reduce the viscosity and density of a given blend. When ethanol content is high in e-diesel blends, the higher heat of vaporization leads to decreased cylinder temperatures which increases the hydrocarbons remaining from combustion. Blends of ethanol-biodiesel-diesel have a significant effect on THC emissions depending on the ethanol blending percentage. Researchers have reported optimal ethanol-biodiesel blends (with regard to THC emissions) to be around 5-10% volume of ethanol[6, 33, 34]. It should be noted that increases in THC emissions favor nucleation of hydrocarbons which contribute to soot formation[18].

2.5 Emissions Control Technologies

Emission reductions can be achieved by controlling the fuel composition, engine conditions, or by removing pollutants from the exhaust gas in post combustion processes. Non-catalytic (thermal) exhaust gas clean-up generally requires residence times greater than 50ms and temperatures in excess of 600ºC [12] and catalytic reduction aims to achieve lower temperatures and shorter residence times. Such options may include catalytic systems, thermal reactors, and traps or filters. For example, lean NO_x traps (a form of NO_x adsorption) are effective up to about 70-80% deNOx efficiency - with further improvements predicted utilizing precious metals [12]. Also, new catalysts which oxidize soot at the catalyst soot interface are emerging in the first

commercial application. In addition, diesel oxidation catalysts (DOC) are able to generate more NO_2 for DPF regeneration at lower temperatures [35].

2.5.1 Exhaust Gas Recirculation

Exhaust gas recirculation (EGR) is a NO_x emission reduction technique used in diesel and gasoline engines. The focus here will be on its use in a diesel engine. EGR works by recirculating a portion of an engine's exhaust gas back into the engine cylinders. This serves to replace some of the excess oxygen in the pre-combustion chamber. Because NO_x forms primarily when a mixture of oxygen and nitrogen is subjected to high-temperature, the decreased combustion chamber temperature caused by EGR reduces the NO_x generated. Care must be taken to properly optimize an EGR system or there may be inverse effects such as increase in smoke emissions, increased fuel consumption, or reduced thermal efficiencies[36]. One such mechanism that may be exploited when employing biodiesel blends is the fact that esters undergo decarboxylation of the ester group; this serves to dilute the exhaust gas with more CO_2 than would otherwise be expected from combustion alone[37], aiding to further improve the efficiency of exhaust gas recirculation.

A recent study examined the effect of different blends of diesel-rapeseed methyl esters (RME) with petroleum diesel using EGR. Perhaps most notable from the study, they concluded that a B20 blend of RME employing 20% EGR resulted in a 69% NO_x reduction at the cost of only 7% smoke increase[36]. The results are shown in Figure 11. The legend in Figure 11 corresponds to the EGR rate (0%-20%). The smoke increase at higher EGR was attributed to a decrease of available oxygen leading to incomplete combustion and increased HC emissions. The results also revealed that the effect of EGR was stronger for biodiesel-diesel blends than ternary EBD blends. Compared to biodiesel blends without ethanol, the NO_x emission reduction obtained for ethanol blends were only marginal with increases in EGR [36] (Figure 11).

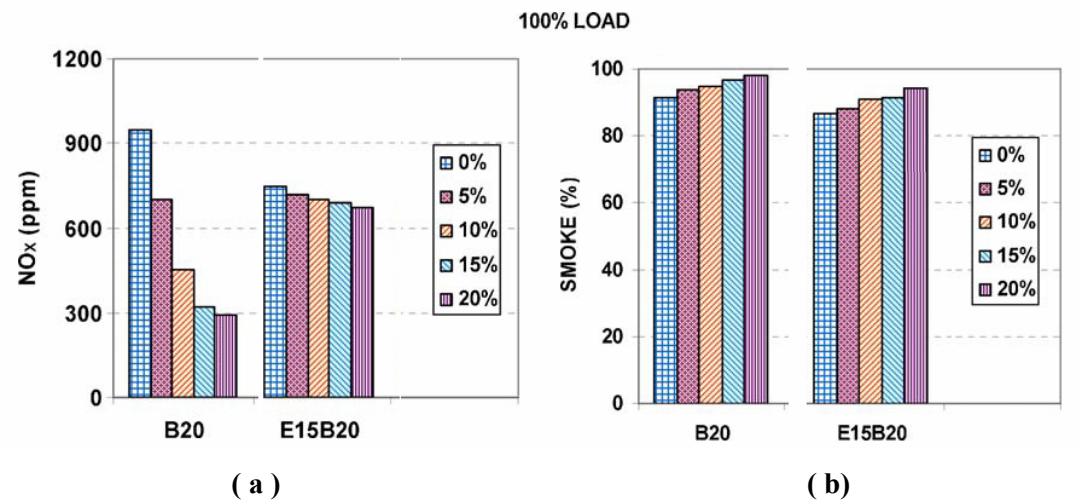

Figure 11. Effect of EGR rate on NOx and smoke [36]

It is believed that further improvements can be achieved by optimizing injection timing when using EGR[36]. One last note as seen in Figure 11 (a), the E15B20 blend performed better than the B20 blend with no EGR; likely due to the high latent heat of evaporation of ethanol. This causes the combustion temperature to be reduced, resulting in lower NO_x emissions[36].

2.5.2 Selective Catalytic Reduction

NO_x controls are also focusing on selective catalytic reduction for diverse applications. Currently, SCR is the leading NO_x control strategy for light and heavy-duty application and works by reducing NO_x on a selective catalyst using an ammonia reductant. The major components of the process are hot exhaust, diesel exhaust fluid and a catalytic converter - where the diesel exhaust fluid is a solution of purified water and urea. The ammonia can come from in-exhaust dissociation of urea, $(NH_2)_2CO$, an organic nitrogen compound that turns to ammonia when heated [35]. Urea injection temperatures less than 190ºC can cause incomplete evaporation of the urea and build up of solid deposits in the injection system[35]. Urea injection quality and mixing are also important. Optimized operation of zeolite SCR catalysts depends on control of adsorbed urea and using oxidation catalysts to deliver proper NO_2 / NO ratios. Cu-zeolites and Fe- zeolites are two of the common materials used in the SCR system. Emerging SCR systems are beginning to incorporate the catalyst onto the diesel particulate filter, however, good DPF regeneration is needed to prevent deterioration of the catalyst [38].

In recent years, low loading Ag/Al_2O_3 catalysts have emerged as a potential interest due to their active and selective nature for N_2 production using a variety of different hydrocarbon feeds[39]. Under typical lean burn engine exhaust (150-300ºC) the NO_x reduction is too low, but with the addition of a small amount of hydrogen the performance was shown to dramatically improve[39]. These systems are being referred to as hydrogen assisted hydrocarbon selective catalytic reduction (HC-SCR). It appears that the hydrogen effect is limited to Ag-based catalysts, but is very much dependent on the support used - with Ag/Al_2O_3 showing the most promise[39]. It is shown in Figure 12 that the promotion effect of hydrogen over Ag/Al_2O_3 on NO_x reduction can significantly lower the temperature required for NO_x conversion[40].

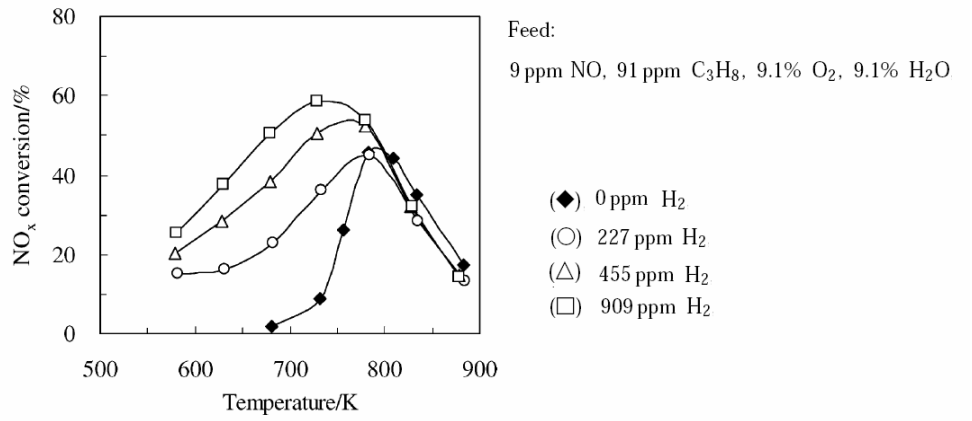

Figure 12. Effect of H_2 on temperature dependence of NO conversion over Ag/Al_2O_3 [40]

SCR is not always the preferred NO_x reduction technology depending on the application. Problematic handling of urea, for example, prevents SCR in many non-road applications. Also, due to the fixed costs of on-board systems, small lean NO_x traps (LNT) are generally cheaper in engines less than 2.0 to 2.5 liters [35]. One last consideration is that mixed-mode engines already have great potential for low-load NO_x reduction, allowing lean NO_x traps to focus on NO_x entering at temperatures greater than 300ºC, thus reducing the precious metal requirements. In this case again, LNTs are currently more economically attractive than SCR systems [35].

2.5.3 Lean NO_x Traps

Lean NO_x Traps LNTs work by storing NO_x as a nitrate on alkali earth metals (such as barium oxide (BaO)) during lean conditions. It acts as a NO_x adsorber and was designed to avoid the problems of EGR and SCR. The zeolite traps the NO and NO_2 molecules—in effect acting as a molecular sponge. Once the trap is full, no more NO_x can be absorbed, and it is passed out of the exhaust system. About every minute, under slightly rich conditions the nitrogen dissociates and releases the NO_x which is then converted on a three-way rhodium catalyst[35]. LNTs can be combined with SCR catalysts, where the SCR is downstream of the LNT. The downstream SCR stores ammonia that is generated in the LNT during rich operation. This ammonia can react with rich or lean NO_x, thus improving system efficiency or decreasing the platinum metal cost while maintaining constant efficiency[35].

A recent development may allow the use of hydrocarbons (HCs) from the fuel as the reductant instead of urea. This would allow for very little precious metal loading but would require temperatures greater than 300ºC to perform well. This design could work well with mixed-mode engines in which deNOx is only needed at higher engine load operations [35]. Figure 13 shows that at temperatures less than 350ºC, platinum loadings of 75 g/ft^3 are desirable. However, at higher temperatures, there is a drop off in efficiency. Therefore, applying low-NO_x combustion strategies up to exhaust temperatures of 350ºC can save on deNOx costs [35].

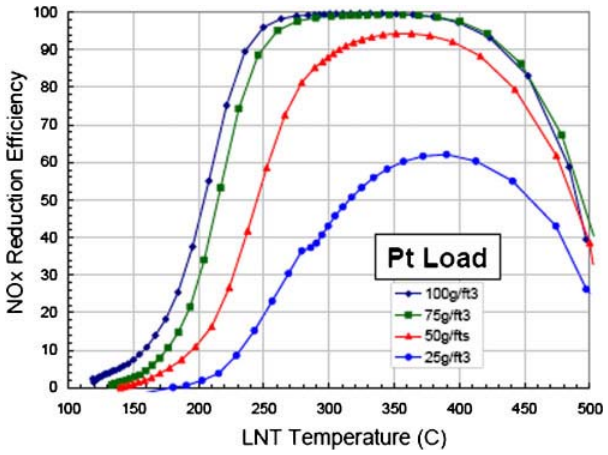

Figure 13. LNT performance dependency on Pt loading and temperature [35]

2.5.4 Diesel Particulate Filters

Particulates in the exhaust gas stream can also be removed directly via diesel particulate filters (DPF). A diesel vehicle with a functional filter will emit no visible smoke from its exhaust. Unlike a catalytic converter, which is a flow-through device, a DPF cleans exhaust by forcing the gas to flow through a filter. A method must exist for the DPF to clean itself since mass accumulation and an increase in exhaust manifold pressure during DPF operation are a concern. The DPF may either burn off the accumulated particulate matter with the aid of a catalyst (passive design), or actively heat this filter soot to combustion temperatures[12]. Engine modifications may either heat the exhaust gases or produce high amounts of NO_x which would subsequently oxidize the particulates at relatively low-temperatures. Increases in NO_2 production can enhance passive soot oxidation at lower temperatures[35, 36].

It has been observed by researchers that the oxidative reactivity of soot formed from different fuels can vary. Biodiesel soot, for example, has been shown to exhibit higher oxidative reactivity than soot derived from conventional diesel and has been attributed to the higher oxygen content of biodiesel[41, 42]. Because thermal regeneration on DPFs requires exhaust temperatures to be >500ºC, the increase in biodiesel soot reactivity has important real-world application potential in the regeneration of DPFs. Exploitation of this phenomena requires an understanding of the low-temperature oxidation chemistry of oxygenated blends such as biodiesel and ethanol. A part of the current study is aimed at using biodiesel surrogates and ethanol to explore the low-temperature oxidation pathways of EBD blends.

2.6 Soot Formation

Soot particles form primarily by pyrolysis of heavier fractions in diesel fuel; thus, formation generally begins with a fuel molecule containing 12 to 22 carbon atoms and a H/C ratio of about 2.0, and ends with particles typically a few hundred nm in diameter and having a H/C ratio of about 0.1 [12]. At low-temperatures, aromatic hydrocarbons produce soot via a relatively fast and direct route that involves condensation of the aromatic ring into polycyclic aromatic hydrocarbon structures. Above 1800K, however, a slower, less direct route is favored

that entails ring breakup into smaller hydrocarbon fragments which then polymerize to form larger unsaturated molecules that ultimately produce soot nuclei[12]. Aliphatic molecules predominant in diesel fuels, in contrast, can only follow the less-direct route. The bulk of the solid phase material is generated by surface growth, which involves the gas-phase deposition of hydrocarbon intermediates on the surfaces that develop from the nuclei[12]. Once particles have formed, particle collisions can cause agglomeration which decreases the number of particles and increases the individual particle size.

2.6.1 Oxidative Reactivity of Soot

In general, the rate of soot oxidation depends on the diffusion of the reactants and products to and from the surface; as well as the kinetics of the reaction. For particles less than one micro meter in diameter, diffusional resistance is low and the soot oxidation process in the diesel cylinder is kinetically controlled[12]. There are many oxygen species in or near the flame that can oxidize soot such as O_2, O, and OH. Oxygen presence in fuels also favors higher oxidation of the hydrocarbons remaining from the combustion process; but tests have shown that oxygen content is not the only parameter effecting total hydrocarbon emissions[18]. Higher heat of vaporization of ethanol, for example, can reduce the combustion temperature which increases the incompleteness of combustion. Nano properties of the molecules can also alter the oxidative reactivity of soot. It is understood that the reactivity of diesel soot is strongly affected by such soot properties as fringe length and curvature of the graphene layers within the soot particles, ordering of the crystalline structure, and surface oxygen content of the soot[41]. More oxidatively reactive soot has been shown to contain smaller graphene layers and has a higher surface oxygen content[41]. Comparisons between Fischer-Tropsch (FT) diesel and biodiesel, for example, showed that biodiesel soot contained more oxygen functional groups and was observed to be more oxidatively reactive than FT soot[41]. Biodiesel soot has also shown to be more reactive than conventional diesel fuel due to the fore-mentioned high surface oxygen content[42]. More oxidatively reactive soot is reactive at lower ignition temperatures and, consequently, lowers the temperature required for regeneration by the DPF[43]. Vander Wal has shown that soot may even have a different nanostructure depending on the origin of the diesel fuel; and that increases in the degree of fuel oxygen leads to increasing degree of amorphous nanostructure within the soot

particle[44]. A recent study by Seong and Boehman[41] noted that oxygen enrichment had a greater effect on soot samples generated from high load than those from low load.

2.6.2 Engine Conditions and Soot Reactivity

In addition to the previously mentioned aspects, conditions such as load and EGR can also be controlled to generate more reactive soot. Soot produced during low engine load, for example, has been show to be more reactive than soot from high engine load[45]. In a recent paper by Al-Qurashi and Boehman[43], it was shown that soot generated under 20% EGR conditions was more reactive than soot generated without EGR; the results of which are shown in Figure 14. Interestingly, it was noted that until 18% conversion, 0% EGR soot (DDC0 curve) was slightly more reactive, however, after that point the 20% EGR soot (DDC20 curve) was greater. They confirmed analytically that the 0% EGR soot is structurally less reactive than 20% EGR soot while the oxygen content was the same.

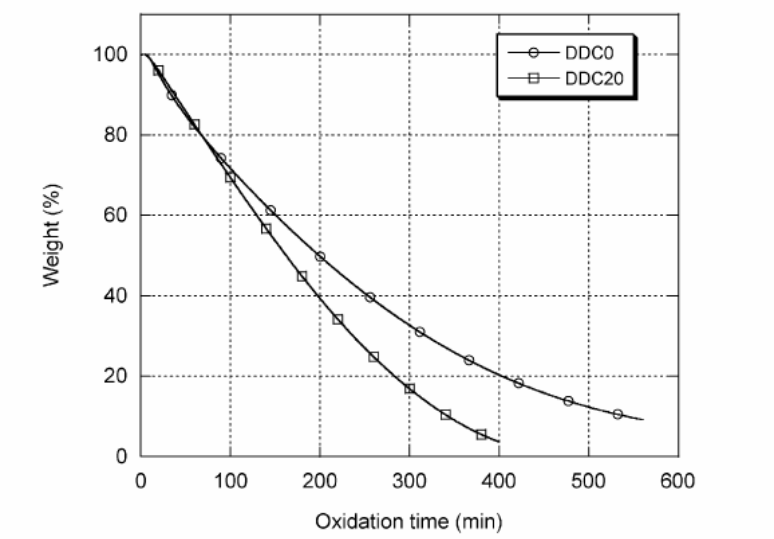

Figure 14. Effect of EGR on soot reactivity (Oxidation temperature: 450 ºC) [43]

2.7 Hydrocarbon Oxidation Chemistry

2.7.1 Oxidation Pathways

In order to understand the oxidation chemistry of hydrocarbon fuels we must first understand the different pathways which exist depending on the temperature regime the fuel is subjected to. This can be broken down into low, intermediate, and high-temperature oxidation. Each consists of initiation, propagation, and termination reactions. Initiation reactions generate an increase in radicals from stable species, such as the decomposition of propane to form methyl and ethyl radicals:

Equation 2. Initiation

$$C_3H_8 \rightarrow CH_3\cdot + C_2H_5\cdot \quad (2)$$

Propagation reactions maintain the number of radical species, for example, a reaction consuming OH radicals and producing ethyl radicals:

Equation 3. Propagation

$$C_2H_6 + OH \rightarrow C_2H_5\cdot + H_2O \quad (3)$$

Termination results in a net decrease in the number of stable radicals, such as the recombination of two ethyl free radicals to produce stable butane:

Equation 4. Termination

$$C_2H_5\cdot + C_2H_5\cdot \rightarrow C_4H_{10} \quad (4)$$

The specific reaction sequences that provide chain branching are subject to change as the temperature, pressure, and reactant composition change[13].

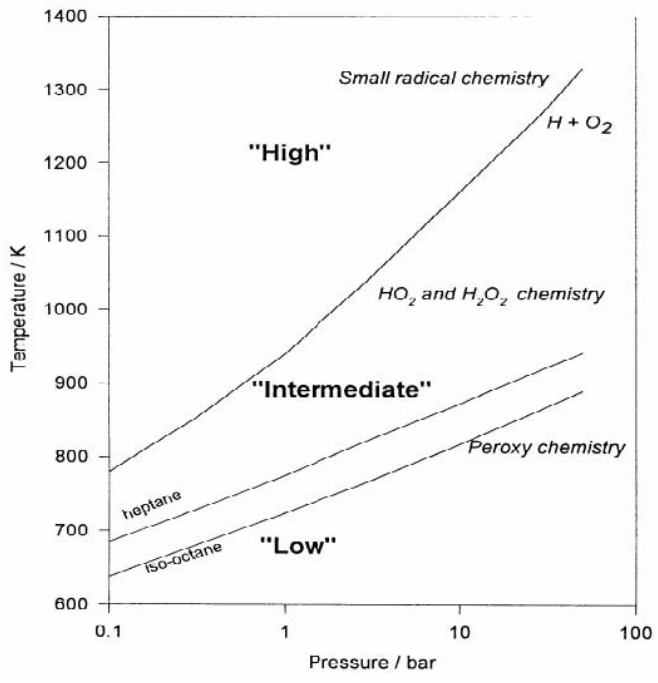

Figure 15. Hydrocarbon oxidation chemistry temperature regimes [25]

In the low-temperature regime the oxidation of hydrocarbons is a complex process involving different propagation and chain ranching reactions, with peroxy chemistry being the predominant pathway leading to cool-flame behavior. The equilibrium constant for the peroxy reaction (Equation 5) is highly temperature dependant and strongly in favor of RO_2 at low-temperature.

Equation 5. Peroxy Chemistry

$$\cdot R + O_2 \leftrightarrow ROO\cdot \qquad (5)$$

It can be noted that above the lower boundary line in Figure 15 the equilibrium shifts to the left and peroxy chemistry becomes insignificant[46, 47]. Early debates considered aldehydes vs. hydroperoxide (ROOH) as intermediates. While aldehydes are important as fuels in the cool-flame region, it was discovered that RȮ compounds are formed into ROH species which play no important role in low-temperature chain branching[47]. Due to its high endothermicity, the chain initiation reaction is not an important route to formation of the radical R once the system has created other radicals. The important generation step is the radical attack on the fuel, with OH being the primary attacker because it has the fastest rate due to its high exothermic nature owing

to the creation of water as a product[47]. The system for creating radicals comes from Equation 6, where X could represent any radical.

Equation 6. Low-temperature system of radical creation

$$RH + X \rightarrow R + XH \quad (6a)$$

$$RH + \dot{O}H \rightarrow R + HOH \quad (6b)$$

It is the fate of the hydrocarbon radical in Equation 6 that determines the existence of the negative temperature coefficient and cool-flames[47]. Here, the H abstracted from RH to form radicals comes from a preferential position, the weakest C-H bond, which occurs on the tertiary carbon atom from the end of the chain[47]. If such carbons exist, O_2 will preferentially attack this position and if there is no tertiary carbon the attack will occur on the next weakest C-H bond, the second carbon.

The intermediate reaction pathway is located between the upper and lower boundary lines in Figure 15. In this regime the high-temperature oxidation pathways (β-scission and H-abstraction) still have too high an activation energy and peroxy chemistry is suppressed as Equation 5 shifts to the dissociation of peroxy radicals, RO_2[46]. The result is a slower fuel consumption rate than low or high-temperature oxidation. The intermediate regime has been termed the negative temperature coefficient (NTC). A pronounced feature of intermediate temperature ignition is the accumulation of H_2O_2 until favorable conditions for its dissociation are reached at adequate temperatures - at which point rapid fuel consumption occurs by attack of OH radicals[47, 48].

In the high-temperature oxidation of large paraffin molecules the initiation step occurs when a C-C bond is broken and hydrocarbon radicals are formed[47]. Recall that C-C bonds (~350 kJ/mol) are substantially weaker than the C-H bonds (410 kJ/mol) in the molecule. The most important high-temperature initiation reaction occurs when these radicals subsequently decay into olefins and H atoms . This initiation step provides the H atoms that can react with oxygen in the system in order to begin the chain branching propagation sequence that supplies the radical pool of OH, H, and O (Equation 7).

Equation 7. High-temperature Chain Branching

$$H + O_2 \rightarrow O + OH \quad (7)$$

Once the radical pool is formed the consumption of fuel is controlled by reactions in Equation 8.

Equation 8. High-temperature fuel consumption by the radical pool

$$RH + OH \rightarrow R + H_2O \quad (8a)$$

$$RH + X \rightarrow R + XH \quad (8b)$$

2.7.2 Suitable Biodiesel Surrogates

As the carbon number of the molecule increases the reactions can become very complex and the number of isomers of the same homologous class of molecules and radicals increase[49]. Crude oil based diesel fuels consist of hundreds of individual components and biodiesel fuels can be made from a wide variety of plants and animals. This complexity leads researchers to search for suitable surrogate compounds to simulate real world biodiesel fuels. Surrogates are simple representations of fully blended fuels comprised of select species of known concentration and exhibit combustion properties similar to the real fuel. Through the use of surrogate fuels the fuel properties and reaction mechanisms become traceable. Earlier research turned towards the short chain ester methyl butanoate ($C_5H_{10}O_2$) as a potential biodiesel surrogate. It was chosen because it was a small molecule that could be used in computational studies and had the essential ester functional group of biodiesel. It was originally expected that the alkyl chain length was long enough to allow fast isomerization reactions of peroxy radicals ($ROO\cdot$) key to low-temperature oxidation chemistry. Researchers such as Gail et al. observed, however, that methyl butanoate does not exhibit any significant cool-flame or NTC behavior typical of long chain biodiesel counterparts and concluded that it should not be considered a suitable biodiesel surrogate fuel[23].

This observation leads researchers to seek a fatty acid ester with a longer alkyl chain to act as a biodiesel surrogate for the purpose of studying low-temperature oxidation. Szybist et al. studied the ignition behavior of methyl decanoate ($C_{11}H_{22}O_2$) in a CFR engine and found that it does exhibit pronounced LTHR indicating a suitability as a biodiesel surrogate [24]. The authors noted that CO_2 was formed at an early stage in oxidation and postulated that the formation was a

direct result of decarboxylation of the ester group because CO_2 formation from CO oxidation with OH radicals is suppressed when sufficient amounts of hydrocarbons remain present. With an alkyl group of 10 carbon atoms, it can be seen that methyl decanoate better represented the low-temperature oxidation behavior of biodiesel than methyl butanoate.

Recent studies by Dayma et al., Glaude et al., and Zhang et al. have shown that methyl hexanoate may be the simplest ester that exhibit strong cool-flame behavior[50-52]. Methyl hexanoate has an aliphatic chain length of six carbon atoms and has been shown to exhibit pronounced cool-flame behavior. In addition, the presence of unsaturation at specific locations can be studied, such as the double-bond on the third carbon of methyl 3-hexenoate which was specifically chosen for the current thesis. It has even been observed that the presence of a double-bond closer to the center of the alkyl chain increases the suppressant effect on LTHR[25, 52]. In this research the selection methyl hexanoate ($C_7H_{14}O_2$) and its unsaturated counterpart methyl 3-hexenoate ($C_7H_{12}O_2$) for a blending study with n-heptane and ethanol serves to simulate real world mixture ratios while using surrogates for biodiesel and diesel fuels.

Chapter 3
Objectives and Hypothesis

Objectives

- To confirm the observations from prior studies that the presence of a double-bond (unsaturation) in the aliphatic chain of fatty acid esters will suppress their cool-flame behavior and that the closer the double-bond is to the center of the chain, the greater the suppressant effect.
- Another objective of this study is to observe the autoignition behavior using various blends of ethanol, n-heptane and C7 esters (saturated and unsaturated) in a motored-engine environment. Even though ethanol has a low cetane number and is a poor compression ignition (CI) fuel by itself, there has been recent interest in blending ethanol with diesel fuels in order to incorporate a renewable content.
- An additional objective of this study is to examine the low-temperature oxidation pathways of the fatty acid esters when blended with ethanol. The reaction pathways will be analyzed by GC-MS and GC-FID examination of the exhaust gas samples of each blend, take at a point just after the onset of cool-flame.

Hypothesis

Achieving these objectives will permit the hypothesis of this research to be tested:

- The presence of ethanol in mixtures with fatty acid esters will suppress but not eliminate the presence of cool-flame behavior during autoignition.
- Additionally, it is hypothesized that blends with increasing ethanol content will have a linear effect on the delay of the onset of HTHR.
- Another hypothesis of this thesis is that increasing the ethanol content of the fuel blends will lead to a lower magnitude of LTHR and that the onset of cool flame will occur further after TDC.

Chapter 4
Experimental

4.1 Motored-Engine Setup

This study was conducted using a modified Cooperative Fuels Research (CFR) octane rating engine to observe the oxidation behavior of blends of n-heptane with ethanol and two biodiesel surrogates over a range of compression ratios. The oxidation behavior was characterized by heat-release and product speciation. Additional measurements were taken for cylinder temperature and pressure and CO and CO_2 emissions at each compression ratio. The CFR engine specifications are listed in Table 1. The intake, exhaust, and jacket cooling systems were modified and the spark plug was disabled by previous users. A gasoline direct injector (GDI) mounted 1.5 meters upstream the intake valve controls the amount of fuel injected into the engine. The fuel blends were pumped into a steel gas-tight vessel and subsequently pressurized with helium gas to 700 psi (4.83 MPa). The intake air temperature is controlled via electric heaters which were fixed to 155ºC in order to ensure that the liquid-fuel droplets were completely vaporized and well mixed with the intake air. The mass flow rate of the fuel injected was determined by using calibration curves that were established individually for each fuel blend. The equivalence ratio was then controlled by adjusting the GDI index via an external controller. A schematic of the motored-engine test setup is shown in Figure 16. Because small variations in ambient temperature were found to affect the repeatability of the heat-release results, previous researchers have modified the original cooling jacket system of the CFR engine such that an external heat exchanger permits the tests to be run under isothermal conditions.

Table 1. CFR Engine Specifications

Number of Cylinders	1
Bore (cm)	8.26
Stroke (cm)	11.43
Displacement Volume (cm^3)	611.7
Compression Ratio Range	3.8 - 15.7
Engine Speed (rpm)	600

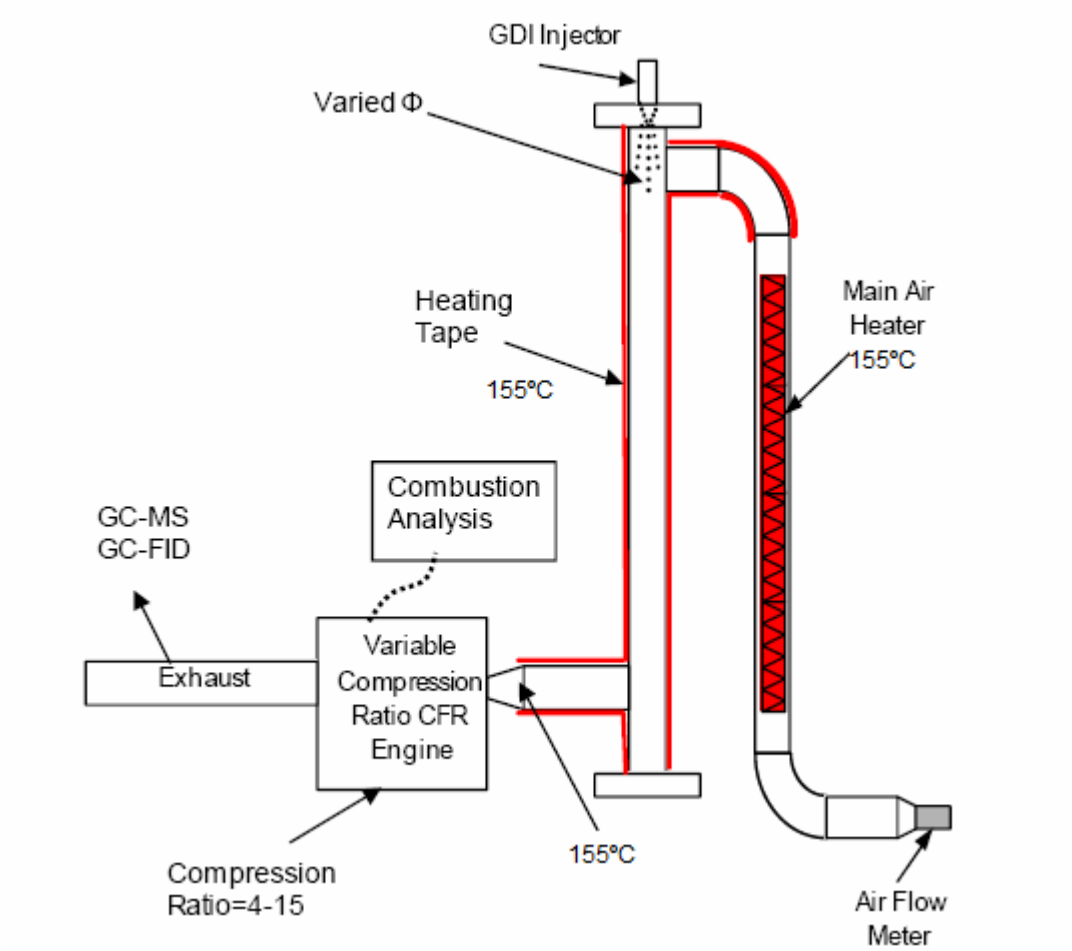

Figure 16. Schematic of the motored-engine test setup (adapted from Yu Zhang [25])

The unique feature of the CFR engine is the ability to vary the compression ratio over a range from approximately 3.8 to 15.7, which provides the opportunity to study the low-temperature oxidation chemistry of fuels over a wide range prior to their autoignition. In addition, the knock meter originally used for octane rating has been replaced with a Kistler 6052B piezoelectric pressure transducer to measure cylinder pressure. An Accu-Coder shaft encoder was used to measure engine speed and to provide a 0.1º crank angle (CA) resolution for the acquisition of cylinder pressure data. Finally, a mass air flow sensor was used to measure the intake air flow rate and temperature sensors were placed along the intake air manifold to ensure that all locations were heated to 155ºC. Labview software was used for data collection.

4.2 Exhaust Analysis

The exhaust system was modified such that exhaust gases could be collected for two separate methods for analysis. The first portion of the exhaust was passed through a chiller and cooled to approximately -5ºC to be sampled utilizing an AVL CEB II emission analyzer. These samples provided real-time information on the carbon monoxide (CO) and carbon dioxide (CO_2) emissions. The second portion of the exhaust was set up to collect samples for subsequent gas chromatography analysis. These analyses would serve to provide information about the stable intermediate products of oxidation. These samples were collected at a compression ratio for each fuel just after the onset of cool-flame. Each sample was cooled to -79ºC, (by means of a dry ice / acetone bath), and passed through a condenser filled with dichloromethane via a vacuum pump. It was determined by previous researchers that most of the condensed intermediate species are stable in a diluted dichloromethane solution and that changes in composition were not expected to occur before the samples could be analyzed via gas chromatography / mass spectrometry (GC / MS).

4.3 Fuel Selection

Four pure fuels were studied in this work: n-heptane, ethanol, and two methyl ester biodiesel surrogates: methyl hexanoate (mhx) and methyl 3-hexenoate (m3h). The four pure fuels were blended into 18 formulations -- listed in Table 2 and graphically represented in Figure 18. The two esters were chosen to study the effect of unsaturation on cool-flame behavior. Specifically, methyl hexanoate was selected because it has a pronounced cool-flame behavior and a chain length of manageable size to study the kinetic mechanism. Because the LTHR is mainly a result of the aliphatic chain, longer esters such as methyl decanoate are likely to over predict this LTHR magnitude. The unsaturated C7 ester (methyl 3-hexenoate) was chosen because unsaturated esters exhibit less LTHR than saturated species and because many real world biodiesel fuels are comprised of multiple unsaturations. n-Heptane was also chosen as a blending component because it is widely accepted as a diesel surrogate fuel because it has a cetane number of 56 and similar combustion properties to crude oil-derived diesel. The blends of mhx and m3h with n-heptane where chosen because, by studying the oxidation of these mixtures,

the interaction between diesel and biodiesel surrogates in the low-temperature regime can be observed. Finally, ethanol was chosen to observe its suppressant effect on the cool-flame behavior of the biodiesel surrogates with n-heptane; also because of recent interest in blending ethanol with diesel in order to incorporate further renewable components. The ester blends were composed of 30% ester and 70% n-heptane prior to being splash blended with ethanol. It should be noted that the ester and n-heptane mixtures were held at a 30:70 ratio, respectively, and that the ethanol component is denoted with an 'E'. For example, the blend denoted E10mhx30hept70 would be comprised of 10% ethanol with a 30:70 ratio of mhx/n-heptane comprising the remaining balance. To clarify, the blend labeled "e10(mhx30/hept70)" would actually be comprised of "e10mhx27hept63". Binary blends of ethanol and n-heptane are presented as e5, for example, corresponding to 5% ethanol and 95% n-heptane. These nomenclatures can be seen in Table 2 and Figure 18 and will continue throughout this manuscript.

Table 2. Test Blends (18 total)

Pure Fuels	Binary Blends	mhx Blends	m3h Blends
n-Heptane	e5	mhx30 / hept70	m3h30 / hept70
Ethanol	e10	e5 (mhx30 / hept70)	e5 (m3h30 / hept70)
Methyl Hexanoate (mhx)	e15	e10 (mhx30 / hept70)	e10 (m3h30 / hept70)
Methyl 3-Hexenoate (m3h)	e20	e15 (mhx30 / hept70)	e15 (m3h30 / hept70)
		e20 (mhx30 / hept70)	e20 (m3h30 / hept70)

Gas chromatography–mass spectrometry (GC-MS) was performed in order to verify the double-bond position in the methyl 3-hexenoate fuel prior to experiments; the results of which are displayed in Figure 17. As a note to the reader, 3-hexenoic acid is another name for methyl 3-hexenoate.

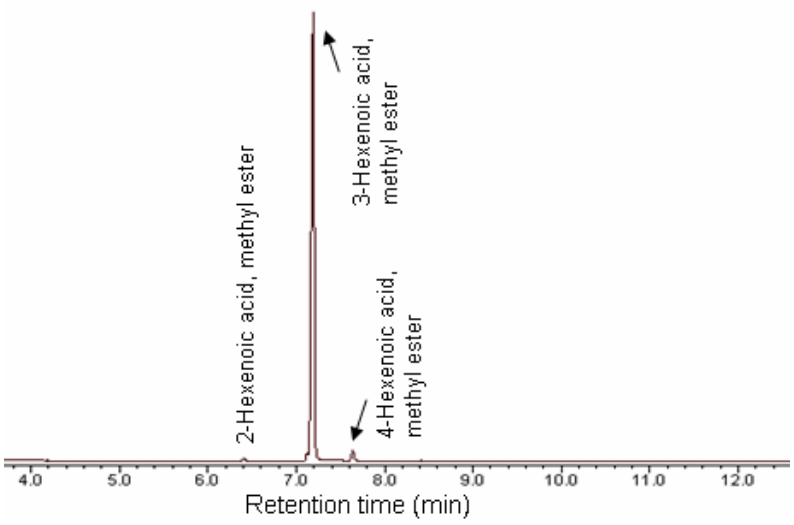

Figure 17. GC-MS of Methyl 3-Hexenoate verifying the double-bond position

Molecular structures and the normal boiling points of the neat test fuels are listed in Table 3.

Table 3. Molecular Structure and Normal Boiling Points of Test Fuels

Compound	Formula	Boiling Point (°C)	Structure
n-Heptane	C_7H_{16}	98.42	
Methyl Hexanoate	$C_7H_{14}O_2$	151	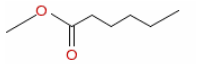
Methyl 3-Hexenoate	$C_7H_{12}O_2$	169	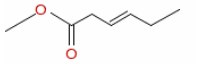
Ethanol	C_2H_5OH	78	

Figure 18 shows the blends tested, where the solid circles represent n-heptane and ethanol binary mixtures while the open circles represent the ester blends. Each open circle corresponds to two separate blends -- one of each of the methyl esters.

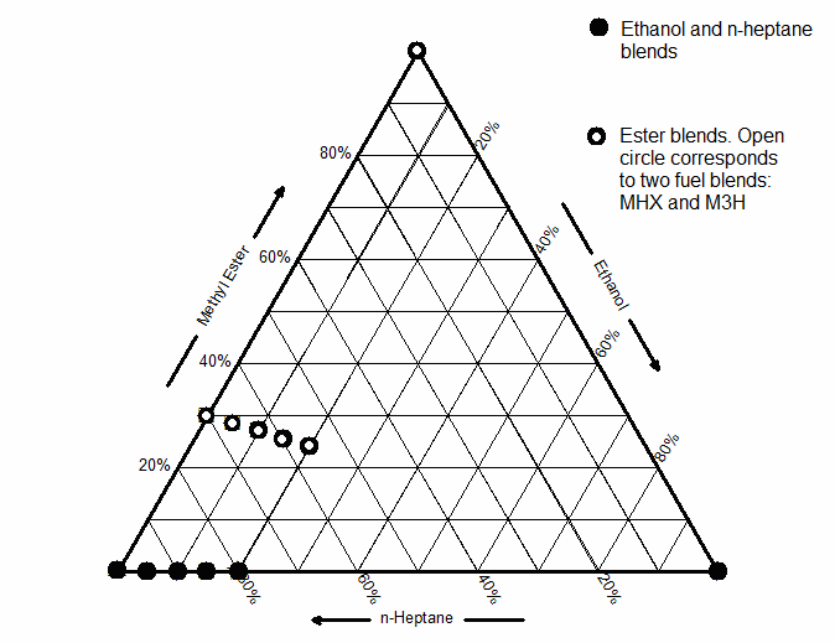

Figure 18. Test Fuels Chart

4.4 Test Conditions and Methodology

In this study, the engine speed was kept constant at 600 rpm for all of the blends tested. The intake pressure is near atmospheric. Each test was performed by starting the compression ratio at the lowest point to guarantee that no low-temperature reaction took place at the initial measurement. The compression ratio was then gradually increased until significant high-temperature heat-release (i.e., ignition) was achieved. Data was collected manually in a notebook as well as automatically using Labview software.

Two separate equivalence ratios (Φ) were used in this study, 0.25 and 0.50; and each test blend was run at each equivalence ratio for a total of 36 test runs. There are several reasons for choosing these low ratios. First, it was of interest to test under lean conditions (low Φ) because it is possible to test a wider range of compression ratios in order to observe pre-ignition low-temperature chemistry. In addition, lower equivalence ratios are typical of homogenous charge compression ignition (HCCI) engine conditions. Equivalence ratio of 0.25 was specifically tested such that the results obtained in this study could be directly compared to previous research done by Yu Zhang[25]. Under the ultra-lean Φ=0.25 conditions, however, there is some difficulty in

determining the exact point of autoignition. As shown in Figure 19, when the compression ratio is increased at Φ=0.25 the cylinder temperature and pressure increase linearly with respect to compression ratio prior to HTHR. Near the point of ignition, however, the cylinder temperature and pressure begin increasing non-linearly over a range of about 0.30 compression ratio before autoignition. In contrast, the ignition event under Φ=0.50 is much more abrupt, with an exponential increase in cylinder temperature and pressure over a narrow compression ratio range of approximately 0.05. It is noted that the maximum pressures are higher in the lean mixtures (Figure 19a) which is expected due to the increased oxygen content in the air/fuel mixture.

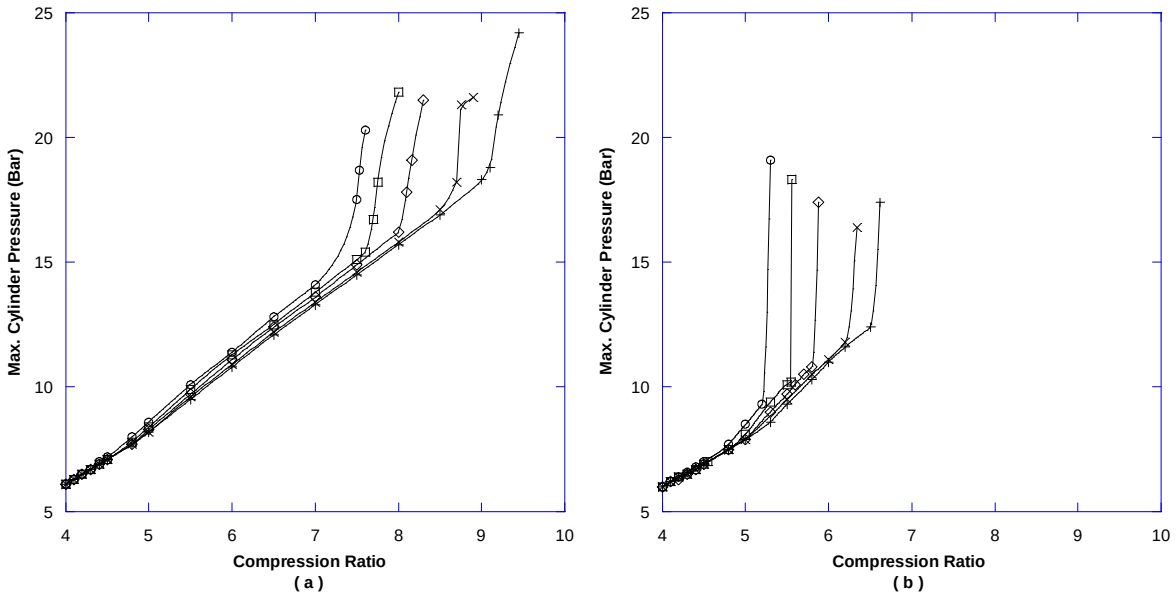

Figure 19. Cylinder pressure comparison between (a) Φ=0.25 and (b) Φ=0.50 of mhx blends: mhx30hept70 (○), e5mhx30hept70 (□), e10mhx30hept70 (◇), e15mhx30hept70 (×), e20mhx30hept70 (+)

For consistency in determining the critical compression ratio (i.e., onset of autoignition) at Φ=0.25, the CO levels were monitored especially closely near the point of autoignition. Just after the onset of autoignition, the CO levels continued to rise for a small range of compression ratio indicating that oxidation is still incomplete at these conditions, as can be observed in Figure 20. Also, during this small window, the CO_2 levels begin to experience a dramatic increase as the CO being produced starts reacting with the OH radicals released from the dissociation of H_2O_2. Note that this occurs because CO is not oxidized to CO_2 until most of the fuel is consumed due to the rapid rate that OH reacts with fuel compared to its reaction with CO[47]. Figure 20 shows the CO and CO_2 emissions of two neat fuels at Φ=0.25 as an example: n-heptane (a) and methyl

hexanoate (b). The autoignition event was chosen at the compression ratio where the first exponential increase in CO_2 was detected and is marked by dashed lines in Figure 20.

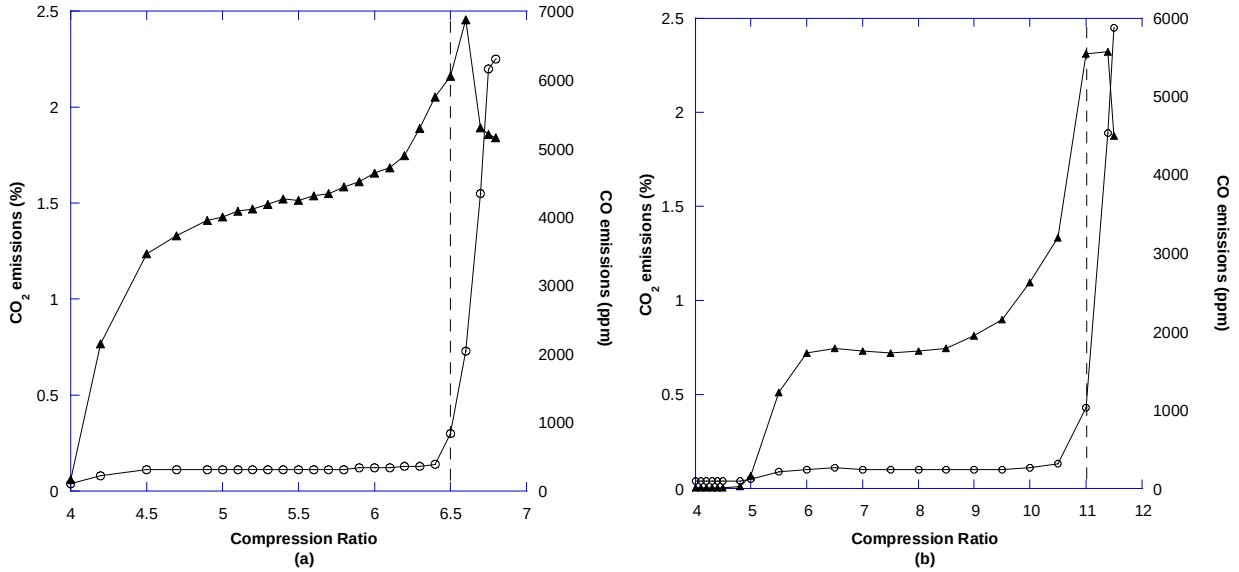

Figure 20. Comparison of CO and CO_2 emissions in order to consistently determine the point of autoignition: CO_2 emissions (○), CO emissions (▲). Example (a) is n-heptane at Φ=0.25 and (b) mhx also at Φ=0.25

As a basis for comparison, the same two neat fuels are shown for Φ=0.50 in Figure 21. It can be noted that the autoignition event occurs much more abruptly (narrower range of compression ratio) at Φ=0.50 than Φ=0.25.

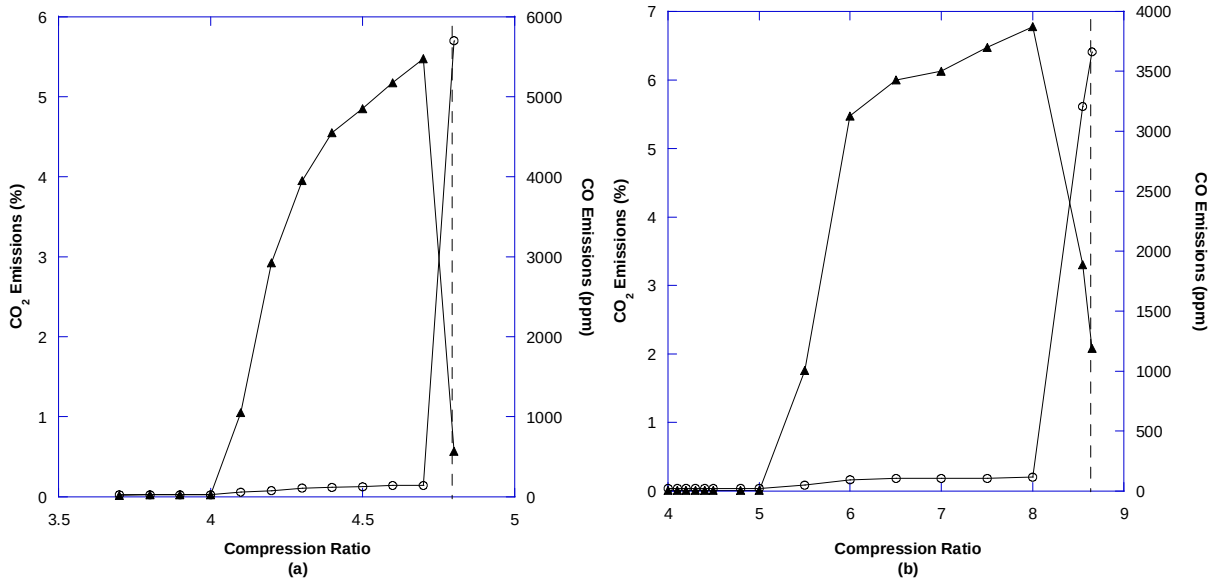

Figure 21. Comparison of CO and CO_2 at Φ=0.50: (a) is n-heptane and (b) is mhx. CO_2 emissions (○), CO emissions (▲)

Chapter 5
Results and Discussion

5.1 List of Critical Compression Ratios

A total of 36 fuel blends were tested in a Cooperative Fuels Research (CFR) octane rating engine. The compression ratio at which each blend reached autoignition is listed in Table 4. Blends with earlier critical compression ratios correspond to shorter ignition delay. Ignition delay is the period between start of fuel injection and detectable ignition; thus, a shorter ignition delay will allow more time for the combustion process to be completed. The order of fuel reactivity of the four neat fuels was as follows: n-heptane >> methyl hexanoate >> methyl 3-hexenoate >> ethanol, with ethanol being the least reactive. The fuels that showed two-stage ignition behavior at the critical compression ratio (CCR) were n-heptane and methyl hexanoate, while ethanol and methyl 3-hexenoate showed only single-stage ignition. This confirms that the saturated ester (mhx) is more reactive than the unsaturated methyl ester (m3h). The ignition behavior can be seen in the heat-release graphs in the following sections.

Table 4. List of Critical Compression Ratios at Intake Temperature 155ºC

Fuel Blend	Φ=0.25	Φ=0.50
n-heptane	6.5	4.8
mhx	11.0	8.7
m3h	12.7	11.4
ethanol	14.5	14
E5 H95	6.7	4.9
E10 H90	7.3	5.3
E15 H85	7.5	5.5
E20 H80	8.0	5.9
mhx30 / Hept70	7.5	5.3
E5 / (mhx30 / Hept70)	7.5	5.6
E10 / (mhx30 / Hept70)	8.0	5.9
E15 / (mhx30 / Hept70)	8.5	6.3
E20 / (mhx30 / Hept70)	9.0	6.6
m3h30 / Hept70	7.8	5.8
E5 / (m3h30 / Hept70)	8.0	6.0
E10 / (m3h30 / Hept70)	8.5	6.1
E15 / (m3h30 / Hept70)	8.8	6.6
E20 / (m3h30 / Hept70)	9.5	7.1

5.2 Low-Temperature Reactivity

In the low-temperature region, CO is primarily produced from the decomposition of aldehydes formed through O_2 addition to the alkyl chain. Because CO is generally an indication of low-temperature oxidation[53], these levels were recorded during testing. An example from the current research shows the CO comparison between three ternary blends with 10% ethanol blended: e10, e10mhx30hept70, and e10m3h30hept70. As shown in Figure 22 (a), ternary blends with the unsaturated methyl ester (m3h) were the least reactive fuel in the lower temperature regime at Φ=0.25, as noted by lower CO emissions prior to autoignition.

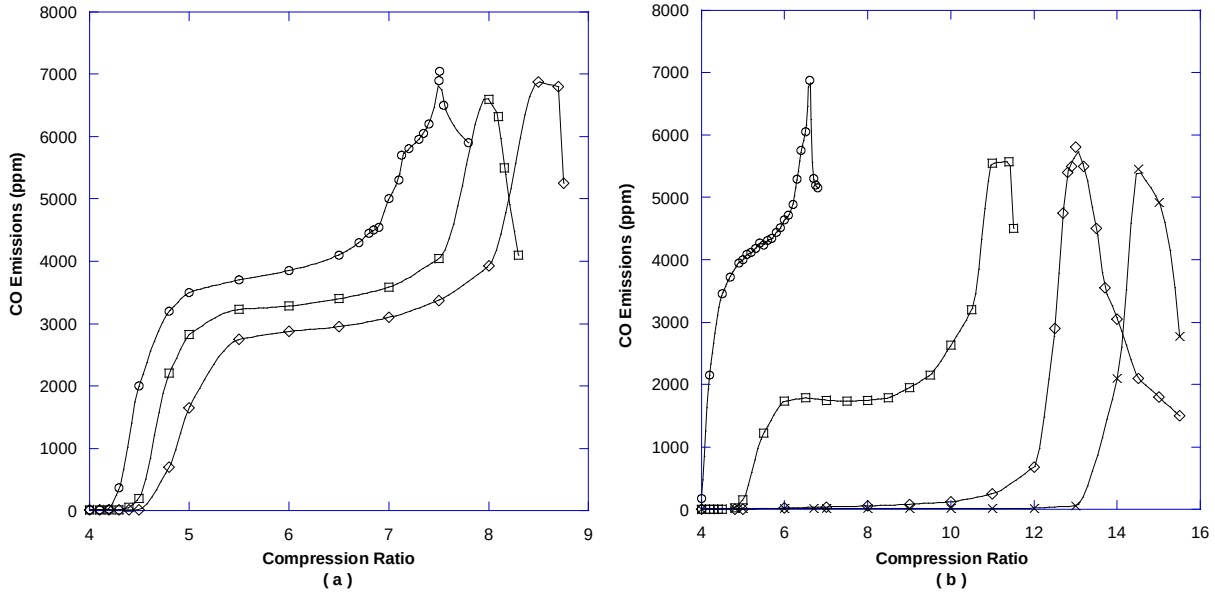

Figure 22. Comparison of CO emissions between e10 blends (a): e10 (○), e10mhx30hept70 (□), e10m3h30hept70 (◇) --- and neat fuels (b): n-heptane (○), mhx (□), m3h (◇), ethanol (×) -- at Φ=0.25

It can also be seen in Figure 22 (b) that the CO emissions from the four neat fuels prior to autoignition are significantly lower for the unsaturated methyl ester and ethanol. The saturated methyl ester and n-heptane are observed to have high CO emissions prior to HTHR. This CO plateau prior to autoignition is an indication of increased low-temperature oxidation reactivity and two-stage ignition.

It has been shown through the research of Zhang et al. [25, 52] that unsaturated ester compounds have less pronounced cool-flame behavior than their saturated counterparts, and that even the location of the double-bond in relation to the ester group can affect the low-temperature

heat-release. The closer the double-bond is to the center of the aliphatic chain, the more resistant the fuel is to low-temperature oxidation. This phenomenon is also observed in alkenes. A study by Tanaka et al. investigated the ignition properties of 1-heptene, 2-heptane, and 3-heptene under lean conditions and found that 1-heptene and 2-heptene showed two-stage ignition and that 3-heptene showed only single-stage autoignition[54]. It is well established that when aromatics or olefins have a long saturated chain, this chain will undergo LTHR while ring structures or compounds with double-bonds will not. The effect of unsaturation was further verified by experiment in this research as shown in the heat-release graphs in Figure 23. Note that the saturated ester (a) displays pronounced two-stage ignition while its unsaturated counterpart (b) shows no cool-flame behavior under the same engine conditions. It should be noted that the smaller peak in (a) corresponds to the LTHR. It is likely that the LTHR observed in Figure 23a is the result of low-temperature oxidation of the aliphatic chain and that the ester group does not participate. Thus, it is apparent that the presence of a double-bond in the aliphatic chain suppresses cool-flame behavior and in turn leads to a delay in onset of autoignition. This is explained because the double-bond inhibits isomerization reactions of peroxy radicals (ROO·) that are key in low-temperature oxidation chemistry. Also, it can be noted that the magnitude of HTHR is about an order of magnitude higher than that of LTHR which can be clearly seen in Figure 23a.

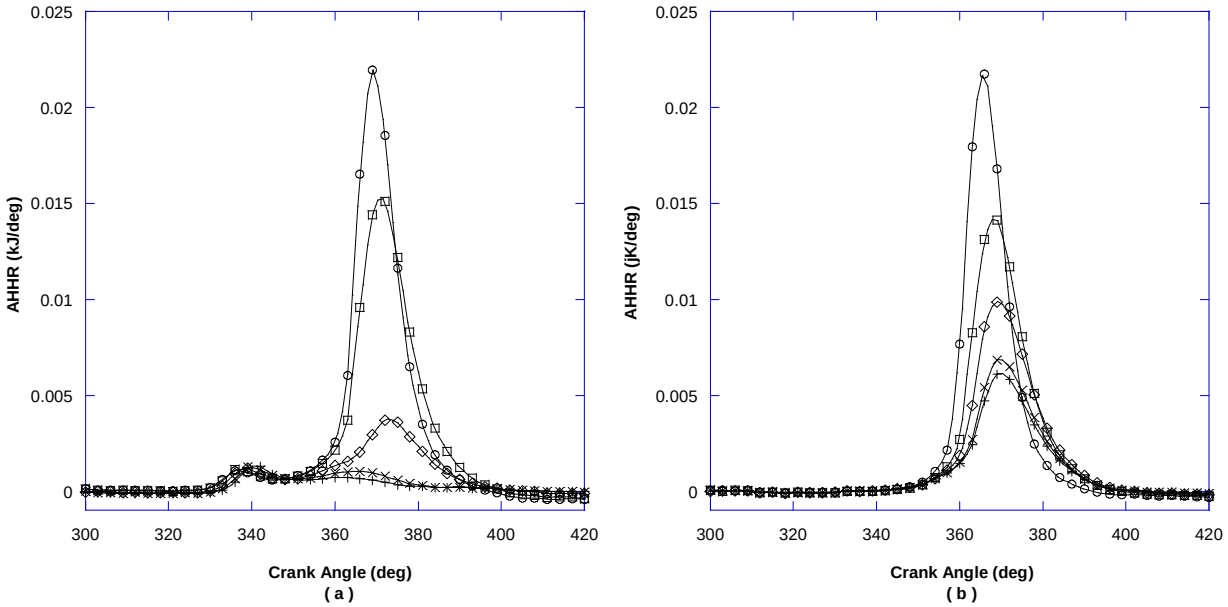

Figure 23. Heat-release rate profiles at different compression ratios for the oxidation of methyl hexanoate at Φ=0.25 ----- (a): 11.50 (○), 11.40 (□), 11.00 (◇), 10.50 (×), 10.00 (+) --- and the oxidation of methyl 3-hexenoate (b): 13.50 (○), 13.20 (□), 13.00 (◇), 12.90 (×), 12.80 (+)

Another objective of this study is to further understand the low-temperature oxidation behavior of short chain surrogate biodiesel fuels, namely methyl hexanoate and methyl 3-hexenoate with blends of ethanol and n-heptane (chosen as the diesel surrogate). The heat-release graphs in Figure 24 show the progressive change in ignition behavior of mhx/n-heptane and its ethanol blends at Φ=0.50.

Several trends are observed from this data. It can be observed that the onset of LTHR occurs at an earlier crank angle as the compression ratio is increased for all blends tested. This advance is expected because increasing the compression ratio makes more favorable conditions in temperature and pressure for the decomposition of ketohydroperoxides to occur earlier. Furthermore, it is understood that low-temperature heat-release is initiated by chain branching through the decomposition of these hydroperoxides[13, 25, 46]. Also, the magnitude of the LTHR increases with increasing compression ratio, except the magnitude of the LTHR at the critical compression ratio -- which decreases with increasing ethanol content. Note the LTHR of the E5 blend in Figure 24 (a) compared to the E20 blend (b). The leftmost curve is the compression ratio of autoignition for both (a) and (b). The magnitude of LTHR at autoignition is observed to decrease with additional ethanol content while the magnitudes of the LTHR leading up to autoignition continue to increase. Also, the overall decrease in LTHR magnitude was expected with increasing ethanol content because ethanol, as with methyl 3-hexenoate, suppresses the cool-flame behavior. This is verified in Figure 25 where no cool-flame behavior is observed in ethanol nor m3h.

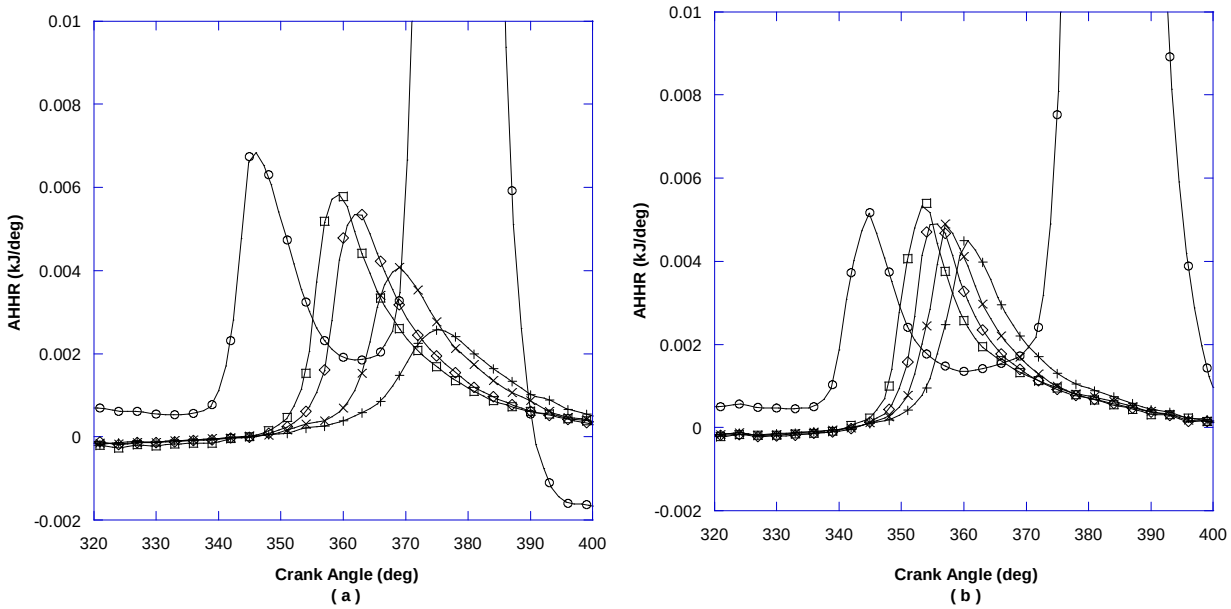

Figure 24. Heat-release rate profiles at different compression ratios for the oxidation of e5mhx30hept70 (a): 5.56 (○), 5.50 (□), 5.30 (◇), 5.00 (×), 4.80 (+) --- and the oxidation of e20mhx30hept70 (b): 6.62 (○), 6.50 (□), 6.20 (◇), 6.00 (×), 5.80 (+) -- both taken at Φ=0.50

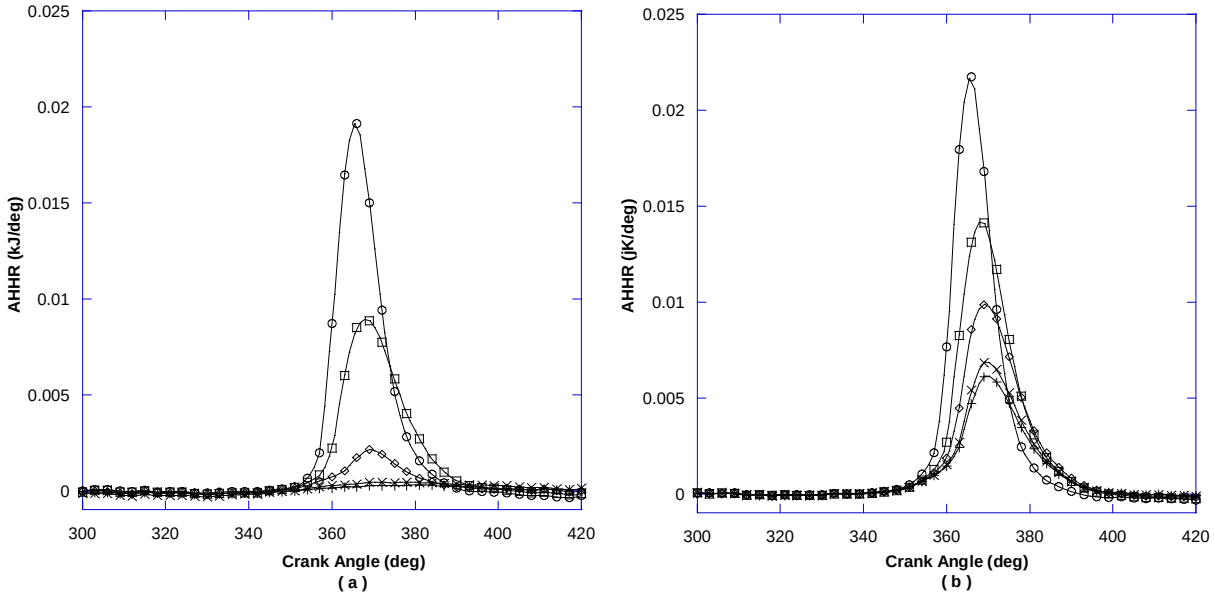

Figure 25. Lack of cool-flame behavior of (a) ethanol and (b) m3h

A different trend is observed when employing neat methyl hexanoate. Here the magnitude of LTHR *decreases* as the compression ratio is increased as depicted in Figure 26. While the decrease in magnitude is very small prior to autoignition, it is clearly lower at the point

where ignition occurs for both Φ=0.25 (a) and Φ=0.50 (b). In this respect, the results for neat methyl hexanoate are similar to blends containing 20% ethanol.

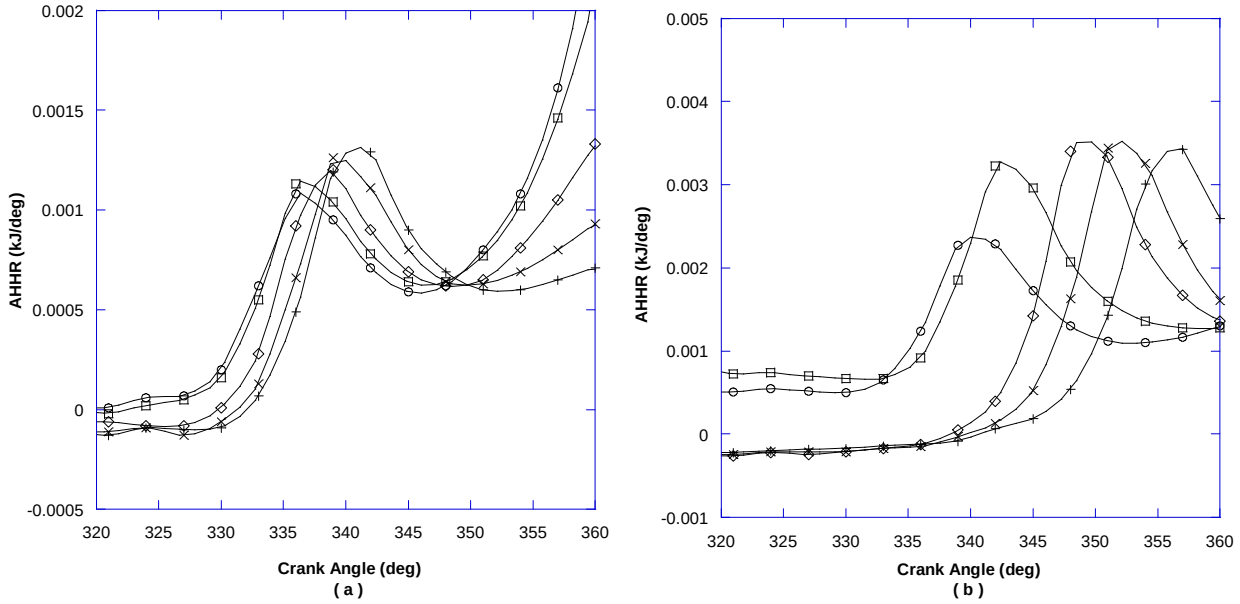

Figure 26. Heat-release rate profiles at different compression ratios for the oxidation of methyl hexanoate at (a) Φ=0.25: 11.50 (○), 11.40 (□), 11.00 (◇), 10.50 (×), 10.00 (+) --- and (b) Φ=0.50: 8.65 (○), 8.55 (□), 8.00 (◇), 7.50 (×), 7.00 (+)

5.3 Effect of Ethanol on HTHR

It was noted that the delay of the critical compression ratio (where the onset of HTHR occurs) is roughly linear with respect to ethanol content. These trends are shown in Figure 27a and Figure 27b. At equivalence ratio 0.25 the methyl hexanoate blends were especially linear. This data indicates that the delay of onset of HTHR due to ethanol content may not be affected by saturation or any functional groups of the parent fuel in the case of methyl esters and n-heptane. Because this research has not tested ethanol blends beyond 20%, or longer methyl ester compounds, trends beyond this regime could not be verified.

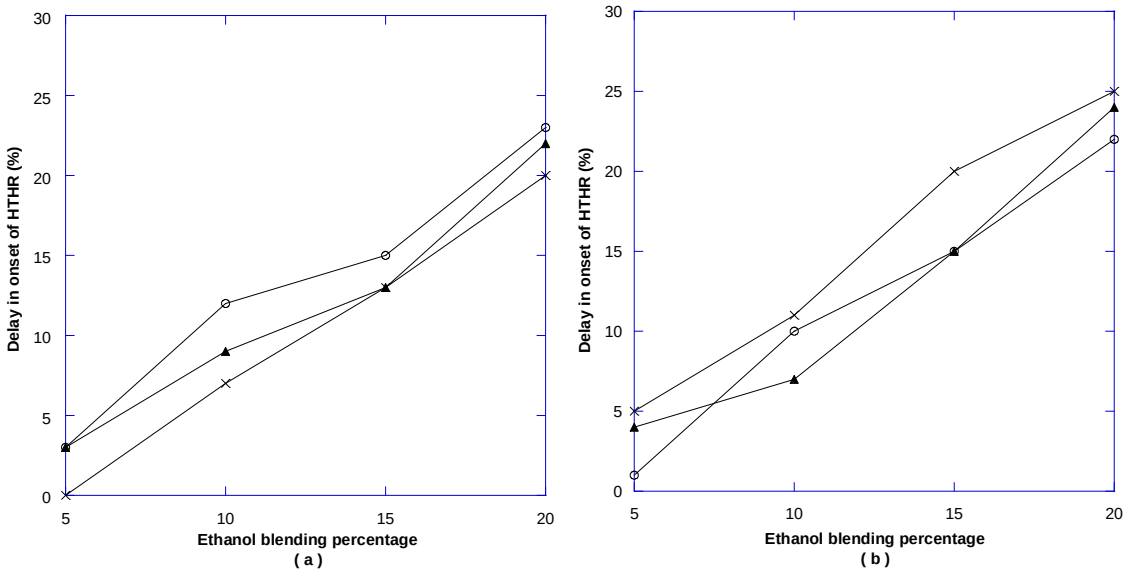

Figure 27. Delay of HTHR as a function of ethanol content: n-heptane (○), mhx blends (×), m3h blends (▲) for (a) Φ=0.25 and (b) Φ=0.50

5.4 General Discussion

This section contains a series of graphs to represent emissions data for CO_2 and CO. The emissions profiles are important because they are a good indicator of where autoignition occurs as well as to give a general idea of the reactivity of the blend. A side-by-side comparison of CO_2 emissions of the three E10 blends reveals that CO_2 emissions at Φ=0.50 are a little more than double that of CO_2 at Φ=0.25 at the critical compression ratio. It is also apparent that because the CCR at higher equivalence ratios is much more abrupt with regard to a range of compression ratios, the CO_2 emissions also increase abruptly at the CCR, as can be noted in Figure 28. A similar observation was shown earlier in Figure 22 where the CO emissions drop off very suddenly at the CCR when the equivalence ratio is higher. At lower Φ (i.e. 0.25) the CO emissions are still relatively high even after the point of autoignition and continue to slowly drop off as the compression ratio is slowly increased. The order of low-temperature oxidation reactivity can also be seen from the following graphs, where earlier increases in CO and CO_2 correspond to more reactive blends. Of the three E10 blends, the order of reactivity is as follows: E10 >> E10mhx >> E10m3h.

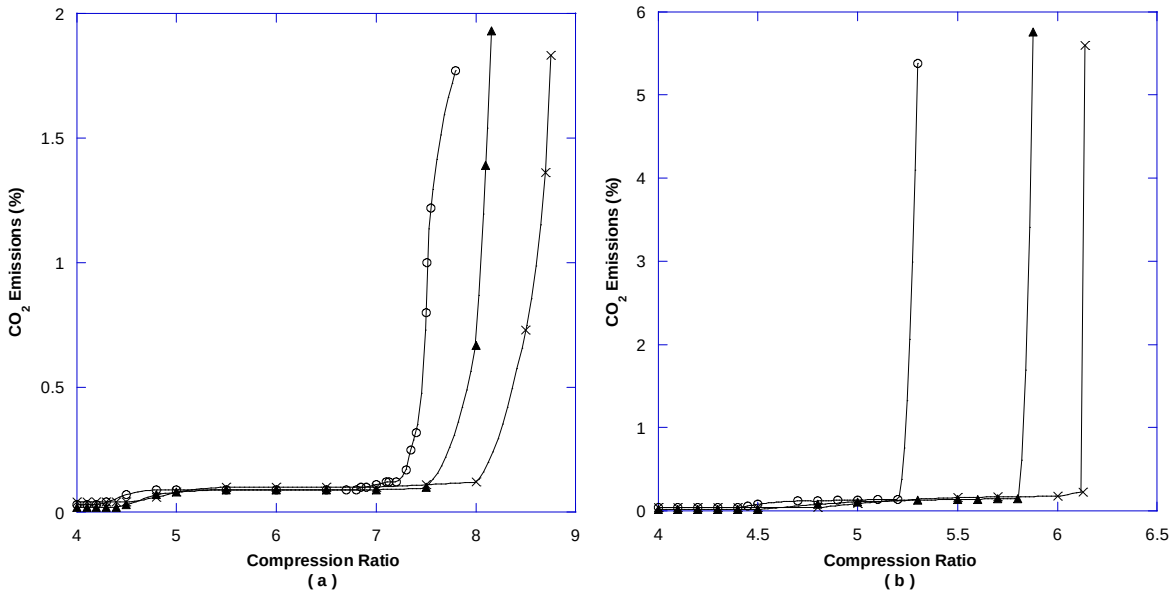

Figure 28. CO_2 Emission of e10 blends: e10 (○), e10mhx30hept70 (▲), e10m3h30hept70 (×) for (a) Φ=0.25 and (b) Φ=0.50

In addition to emissions profiles, temperature and pressure can also be an indicator of when autoignition occurs and the reactivity of a fuel. The E10mhx blend at Φ=0.25 and Φ=0.50 had a peak pressure and temperature lower than that of the E10m3h blend, further verifying that mhx blends were more reactive than m3h blends. These trends are shown in Figure 29 and Figure 30. As with the emissions profiles, the temperature and pressure are more sensitive to compression ratio changes at higher equivalence ratios. Also apparent is that the maximum pressure of the same blends tend to increase with increasing equivalence ratio.

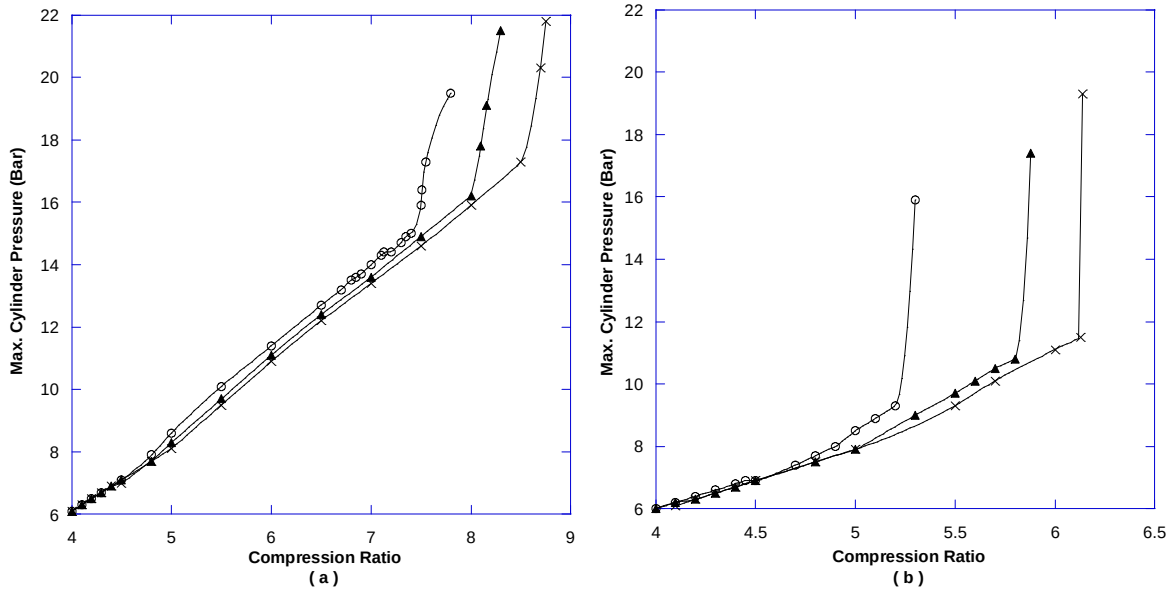

Figure 29. Cylinder pressures of e10 blends: e10 (○), e10mhx30hept70 (▲), e10m3h30hept70 (×) for (a) Φ=0.25 and (b) Φ=0.50

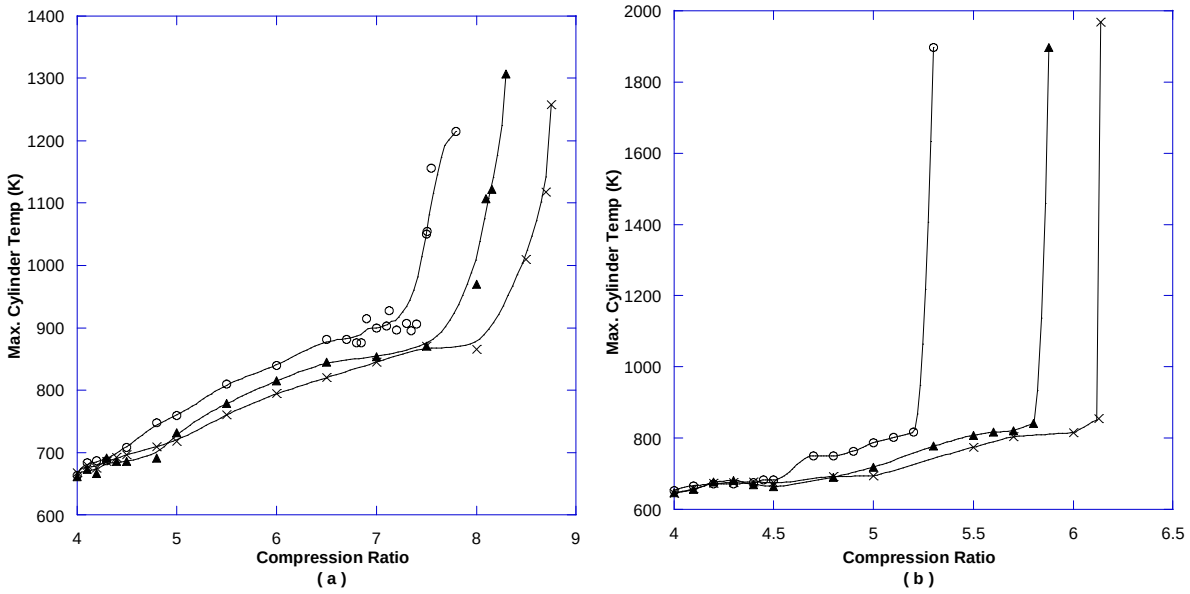

Figure 30. Cylinder temperature of e10 blends: e10 (○), e10mhx30hept70 (▲), e10m3h30hept70 (×) for (a) Φ=0.25 and (b) Φ=0.50

Another trend observed was that blends with increasing ethanol content had a lower magnitude of LTHR and an onset occurring further after top dead center at the same compression ratio, which can be seen in Figure 31. This data indicates that blends with increasing ethanol content are less reactive in the low-temperature regime. In addition, it can be seen that increasing the equivalence ratio from Φ=0.25 to Φ=0.50 causes an increase in the magnitude of the LTHR and also causes the peak LTHR to occur further after TDC when compared to a similar compression ratio.

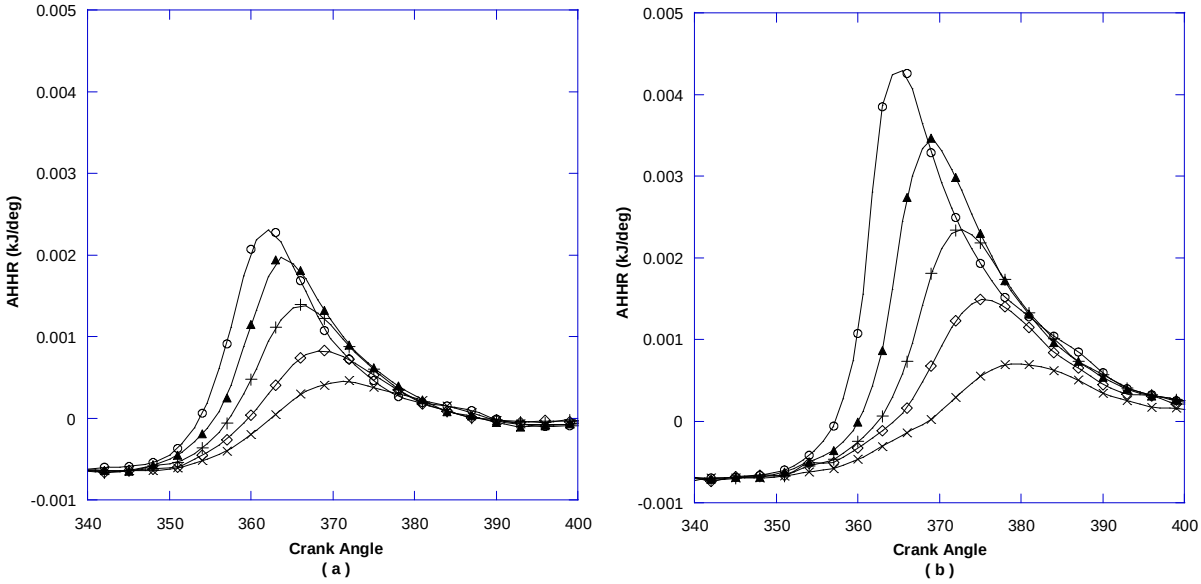

Figure 31. LTHR of mhx and its blends of increasing ethanol percentage at a compression ratio 5.00: mhx30hept70 (○), e5mhx30hept70 (▲), e10mhx30hept70 (+), e15mhx30hept70 (◇), e20mhx30hept70 (×) at equivalence ratios (a) Φ=0.25 and (b) Φ=0.50

5.5 Intermediate Species

The GC-MS analysis of exhaust gases shows a range of intermediate species. Some are typical of low-temperature hydrocarbon oxidation, such as olefins: propene, butenes, pentenes, and heptenes --- and aldehydes: acetaldehyde, propanal, butenals, and pentenals. Other species observed include unsaturated methyl esters: methyl 2-hexenoate, methyl 4-hexenoate, methyl 5-hexenoate, methyl 2-propenoate, and methyl 3-butenoate --- and ketones: 2-butanone, 2-hexanone, 3-hexanone, 2,5 hexanedione, 3-hepen-2-one. The samples also showed unreacted fuel molecules of ethanol, methyl hexanoate/hexenoate, and n-heptane. Since the intermediate

species and oxidation pathways of methyl hexanoate and methyl 3-hexnoate have been extensively outlined in the works of Yu Zhang[25], this section will focus on how these biodiesel surrogates behave differently when blended with ethanol. Different intermediate species exist between the saturated and unsaturated methyl ester blends. For example, the mhx blends contained methyl 3-butenoate while the m3h blends did not. In contrast, the unsaturated ester blends contained toluene while saturated blends did not. It was also noted that the concentration of methyl 2-propanoate was twice as high in the saturated C7 ester blends containing ethanol. These results are displayed in Appendices C - F.

5.5.1 EBD Blends vs. BD Blends

Comparison of the surrogate EBD blends (current work) against surrogate biodiesel-diesel (BD) blends without ethanol (works of Yu Zhang [25]) reveals that certain identifiable intermediate species are present in EBD blends that were not observed in blends without ethanol. Among these and listed in decreasing order of concentration for the mhx blend (appendix C) were: 1,2 propanediol >> cyclohexene >> 2H-pyran-2methanol >> 2H-pyran-tetrahydro-2-dimethyl >> 2-hexen-4-ol-5-methyl >> 2,3 epoxyhexanol >> 1-butanol-3-methyl >> 3-hexanone >> 1-heptanol >> 2,4 pentanedione. Similarly, for the m3h blend (appendix D) the species are listed as follows in decreasing concentration: 1,2 propanediol >> cyclohexene >> 2H-pyran-2methanol-tetrahydro >> 2H-pyran-tetrahydro-2-methyl >> 2-hexen-4-ol-5-methyl >> toluene >> 3-hexanone >> 2-butanone >> 1-heptanol >> 2-hexanone >> 3-hepten-2-one.

5.5.2 Olefins

Yu Zhang[25] noticed in his work with non-ethanol blends that saturated mhx blends generally produced more olefins (propene, 1-butene, 1-pentene, 2-pentene, and 3-heptene) than unsaturated m3h blends. While it was noted in the current paper that *ethanol* mhx/heptane blends still produce more olefins than similar m3h blends, there is a somewhat different trend. The relative differences were compared between ethanol and non-ethanol blends and the results are displayed in Figure 32. It should be noted that a ratio lower than one in Figure 32 and Figure 33 indicates that a given species is present in greater concentration in *m3h* blends than in similar

mhx blends; and a ratio greater than one indicates greater species concentration in *mhx* blends compared similar m3h blends.

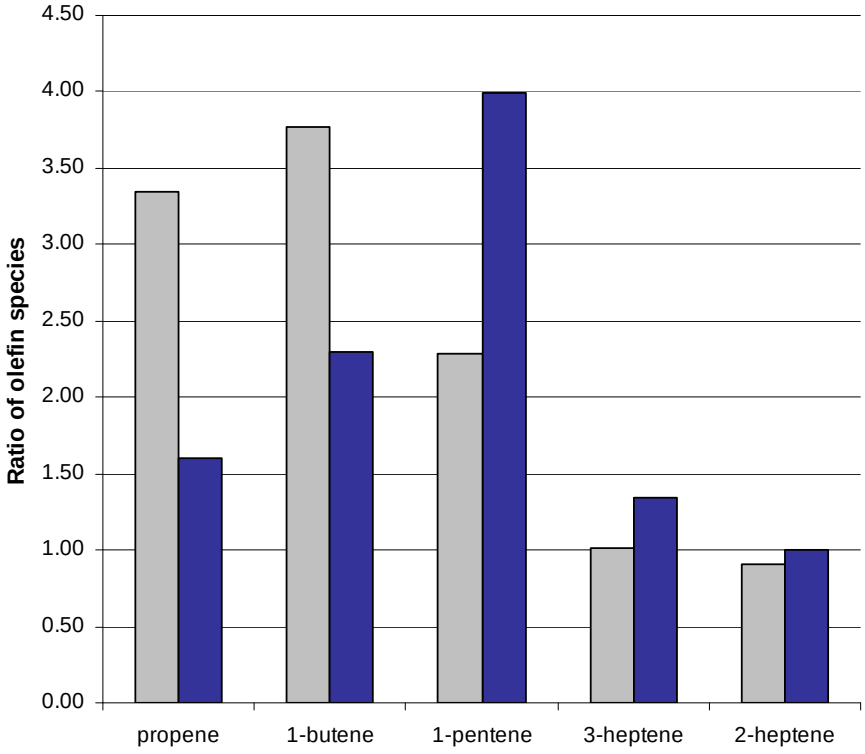

Figure 32. Ratio of the concentration of olefin species produced in the low-temperature regime for mhx blends to the concentration of olefins produced m3h blends.
20% ethanol is added, *e20mhx30hept70* **(■) -- no ethanol is added,** *mhx30hept70* **(■)**

It can be seen in Figure 32 that mhx blends produce significantly more short olefins (propene and 1-butene) than m3h blends when ethanol is present at 20%; and that the relative discrepancy is diminished for longer olefins. Propene is present at more than a 3:1 ratio in mhx blends with ethanol. In contrast, propene concentration in non-ethanol blends is only present at a 1.5:1 ratio in mhx blends as compared to m3h blends. Similar to propene, 1-butene is present at much greater concentration in mhx blends than m3h blends when ethanol is present; and less concentration when ethanol is not in the fuel blend (Figure 32). It can also be seen that the concentration of olefin species produced in the low-temperature regime for 1-pentene is higher in the unsaturated C7 ester blends than the saturated C7 ester blends. These observations would infer that blending ethanol with C7 esters has a significant effect on the ratio of the concentration of olefin species produced in the low-temperature regime for mhx blends to m3h blends for short olefins; while the relative difference in the concentration of olefin species becomes lesser as the

olefin molecules becomes larger (Figure 32). Product distribution of the intermediate species as measured in the current work can be found in Appendix C and D.

5.5.3 Aldehydes

An interesting difference observed between ethanol blends and non-ethanol blends is the relative concentration of acetaldehyde between mhx/m3h blends. The data from Yu Zhang[25] showed a slight increase (10%) in acetaldehyde concentration for mhx blends verses m3h blends (first blue bar in Figure 33). Data from the current work (which incorporates ethanol) shows a quite significant increase in acetaldehyde concentration for mhx blends compared to m3h blends (first grey bar in Figure 33).

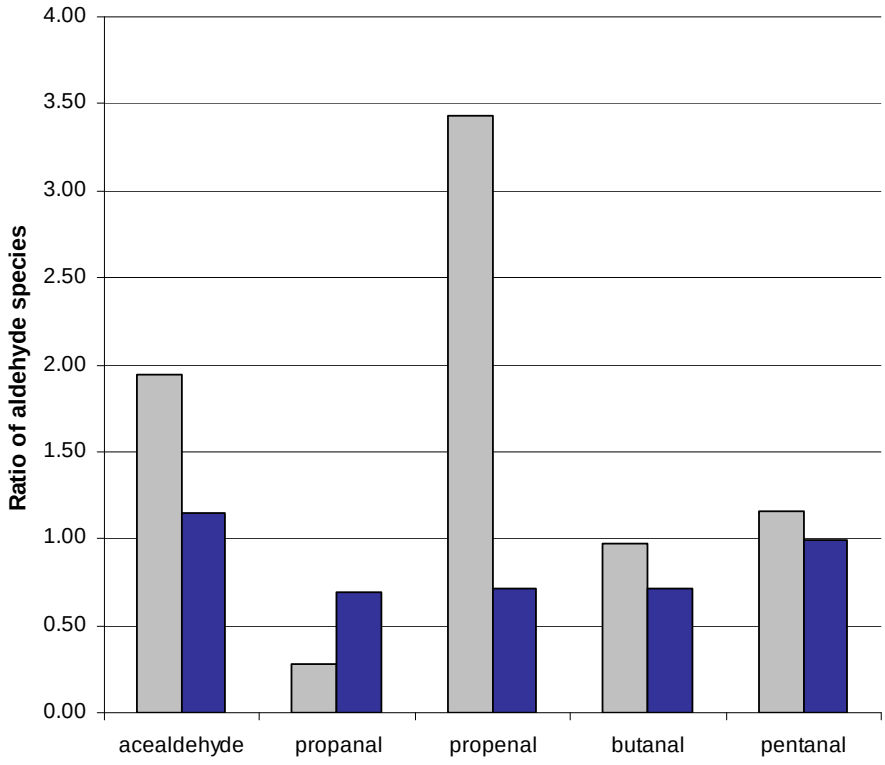

Figure 33. Ratio of the concentration of aldehyde species produced in the low-temperature regime for mhx blends to the concentration of olefins produced m3h blends.
20% ethanol is added, *e20mhx30hept70* **(▒) -- no ethanol is added,** *mhx30hept70* **(■)**

A trend that appears in the aldehydes and not in the olefin species is that propanal and butanal are present at greater concentration in m3h blends than in mhx blends for fuel mixtures with and without ethanol (Figure 33), as can be noted by the ratio being less than one (recall that a ratio below 1 indicates that a species is present in greater concentration in *m3h* than in the *mhx* blend). Most notable from the aldehyde species is propenal (acrolein). When no ethanol is present, it is present at roughly a 0.75:1 ratio in mhx:m3h blends; however, when ethanol is blended at 20% in the fuel mixture, it is present at more than three times the concentration in the mhx blend as in the m3h blend (Figure 33). These observations would infer that blending ethanol with C7 esters has a significant effect on the relative concentration of shorter aldehydes (especially the unsaturated aldehyde acrolein) between mhx/m3h blends in the low-temperature regime and less of an effect on larger aldehydes such as butanal and pentanal with the largest difference occurring in the unsaturated aldehyde. Product distribution of the intermediate species as measured in the current work can be found in Appendix C and D.

Chapter 6
Conclusions and Suggestions for Future Work

In this research the low-temperature oxidation chemistry of a saturated ester (methyl hexanoate) and its unsaturated counterpart (methyl 3-hexenoate) were investigated in a CFR motored-engine with blends of a n-heptane and ethanol. Heat-release and CO trend analysis show that the saturated methyl ester exhibited pronounced cool-flame behavior while the unsaturated ester did not. All blends with ethanol exhibited a linear increase in delay in the onset of autoignition with increasing ethanol content. Even at the maximum ethanol blending percentage, the saturated methyl ester continued to exhibit cool-flame behavior; however, the magnitude of the LTHR was lower and the onset occurred further after TDC at a similar compression ratio when ethanol content increased. An interesting trend observed was that the magnitude of LTHR increased with increasing compression ratio for mhx/hept blends while the magnitude of LTHR decreased for the neat mhx fuel. It was also noted that the magnitude of the LTHR at the critical compression ratio decreased with increasing ethanol content for ethanol/mhx/hept blends as a result of the suppressant effect of ethanol. Product distribution of the intermediate species of low-temperature oxidation revealed several compounds present in ethanol-biodiesel-diesel blends that were not observed in similar blends without ethanol. In addition, there were intermediate species that were observed in the saturated methyl ester blends that were not exhibited in the unsaturated methyl ester blends and vice versa. Further analysis of the current data against the works of Yu Zhang[25] reveal that blending ethanol with C7 esters has a significant effect on the relative concentration of intermediate species in the low-temperature regime between mhx/m3h blends of shorter aldehydes and olefins and less of an effect on longer chains.

The motored CFR engine used in this research is a unique piece of equipment capable of studying the oxidation behavior of hydrocarbons within a wide range of compression ratios and at different intake temperatures. In fact, the same engine is currently being experimented with on the effect of EGR on diesel and biodiesel surrogates. Future work on this engine could include studies on longer chain biodiesel surrogates and other alcohol additives. The critical compression ratio and intermediate species of low-temperature oxidation can be compared against current and past works in order to determine what fuels and their blends are optimally suited for application in the current and future diesel market.

Appendix A: Graphs of CO_2, CO, and Max Cylinder Temp and Pressure at Φ=0.25

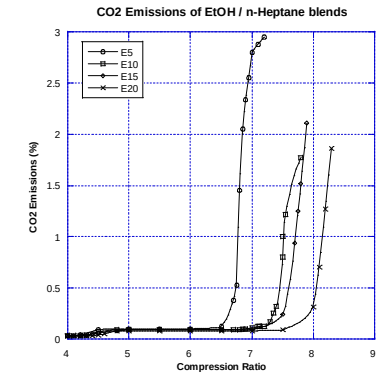

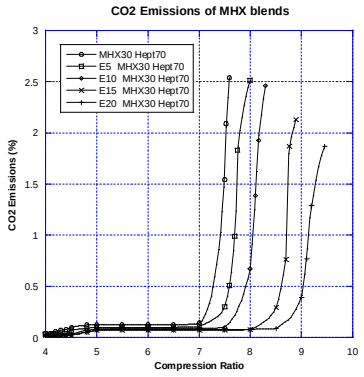

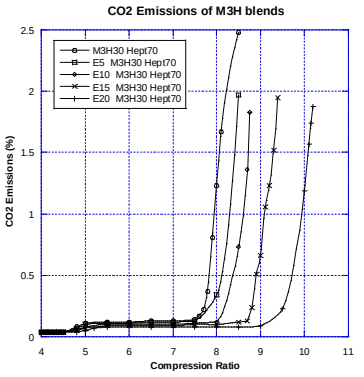

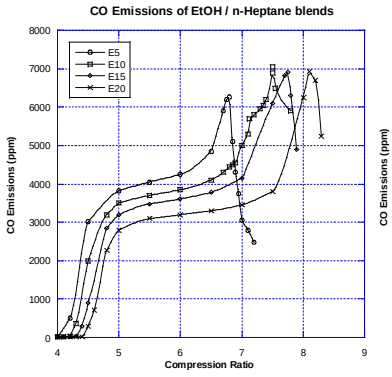

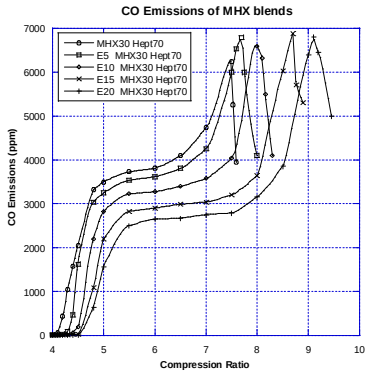

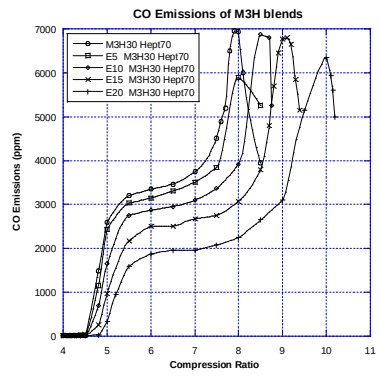

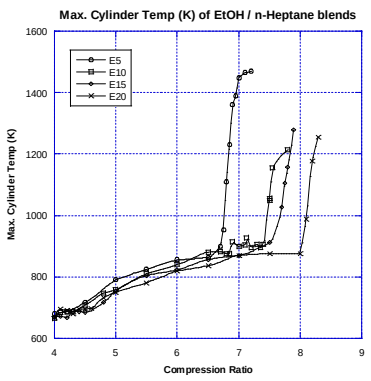

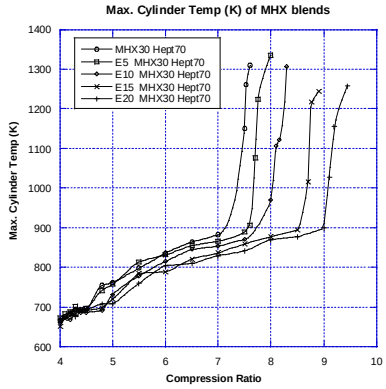

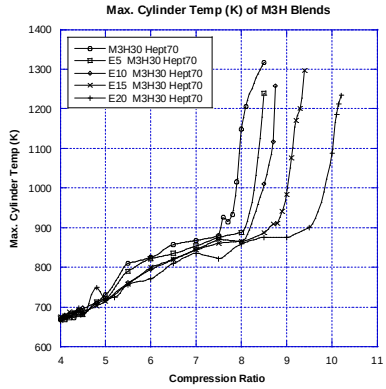

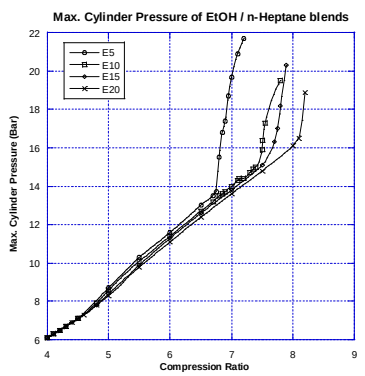

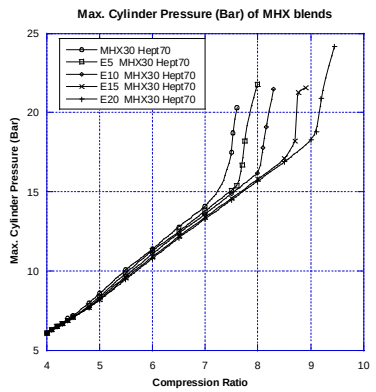

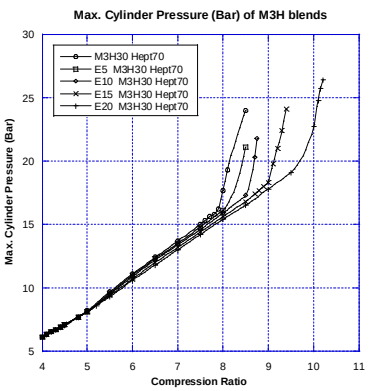

Appendix B: Graphs of CO_2, CO, and Max Cylinder Temp and Pressure at Φ=0.50

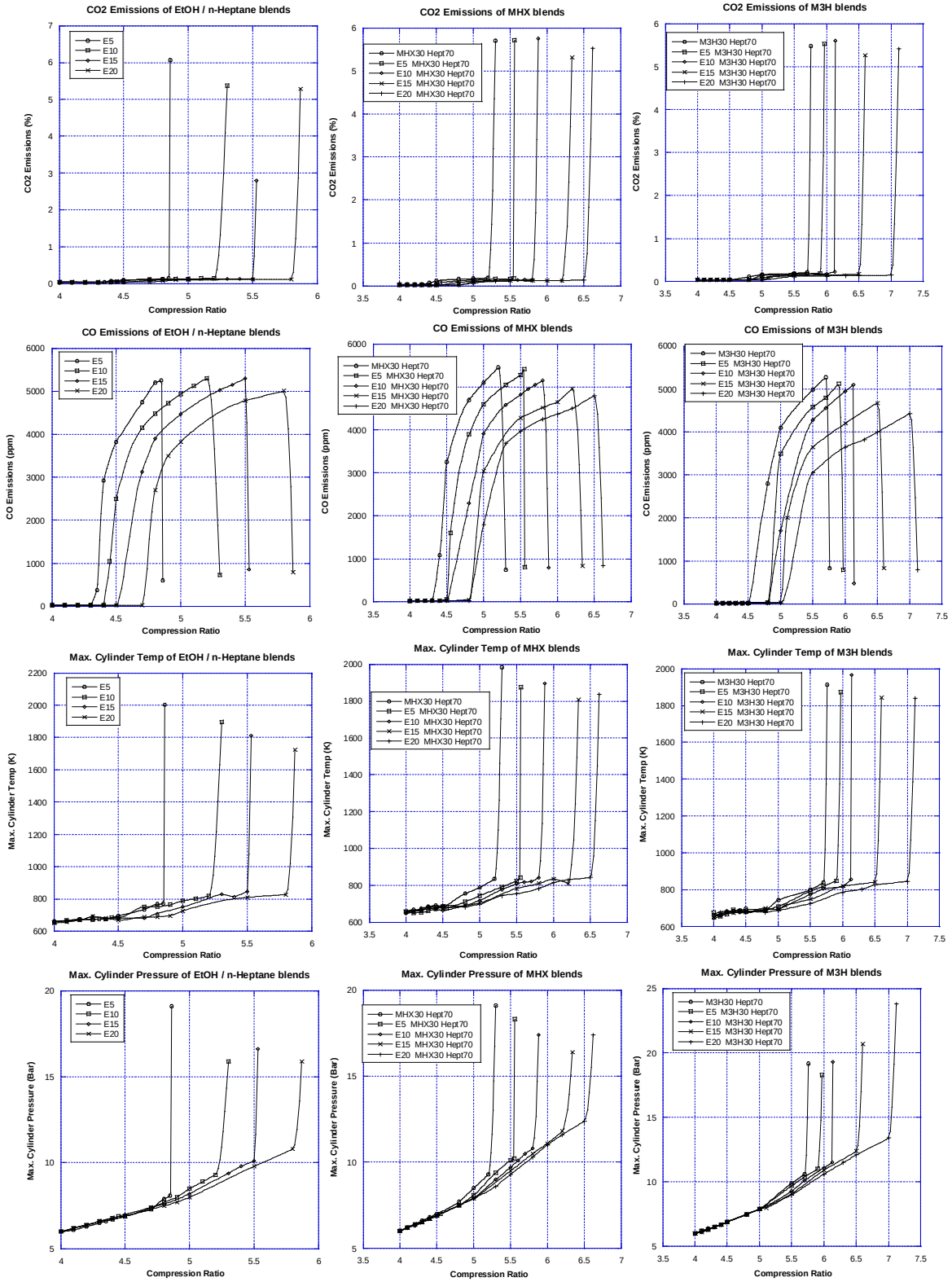

Appendix C

Product Distribution in Low-Temperature Oxidation of the Mixture of Ethanol, n-Heptane, and Methyl Hexanoate e20/(mhx30/hept70)

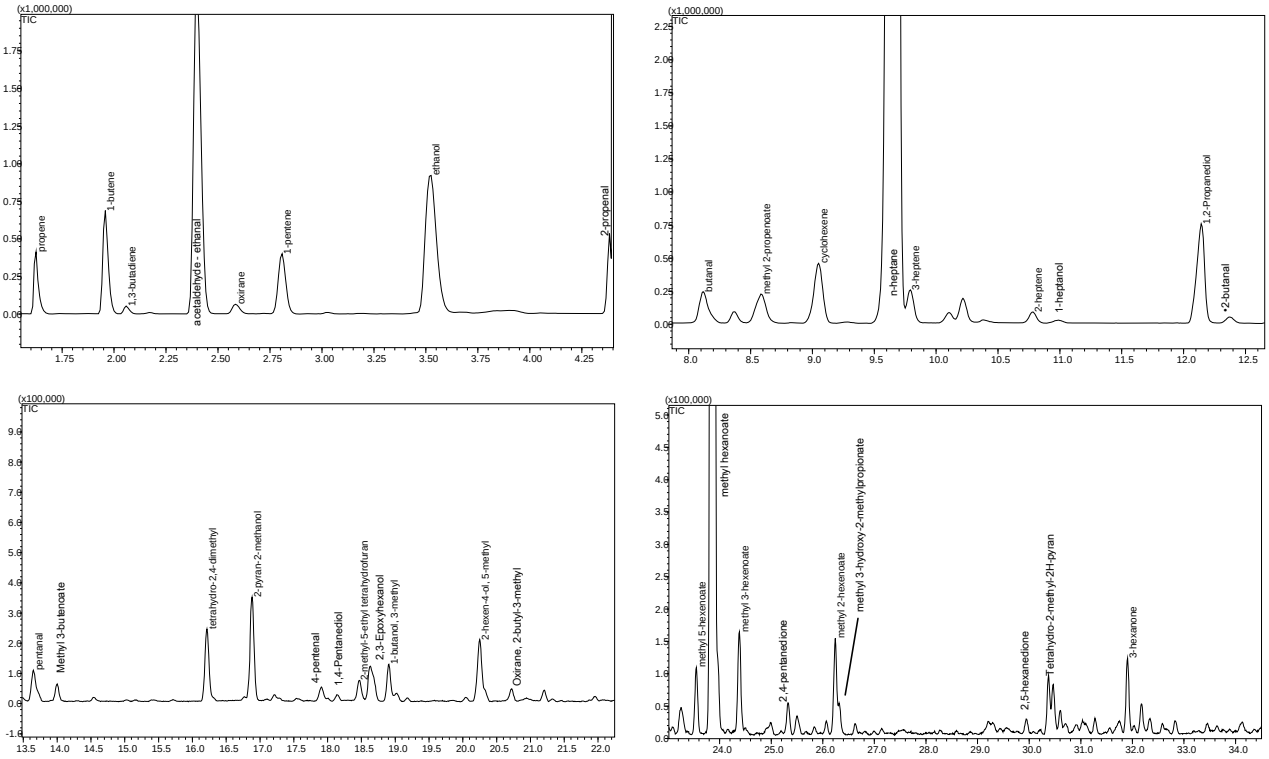

Appendix C: Product distribution in the oxidation of the mixture of ethanol, n-heptane, and methyl hexanoate at compression ratio 5.1. Y-axis represents FID signal strength and X-axis is retention time. Samples were analyzed in HP-5890 GC with injection volume of 1 uL and a split ratio of 30.

Appendix D

Product Distribution in Low-Temperature Oxidation of the Mixture of Ethanol, n-Heptane, and Methyl 3-Hexenoate e20/(m3h30/hept70)

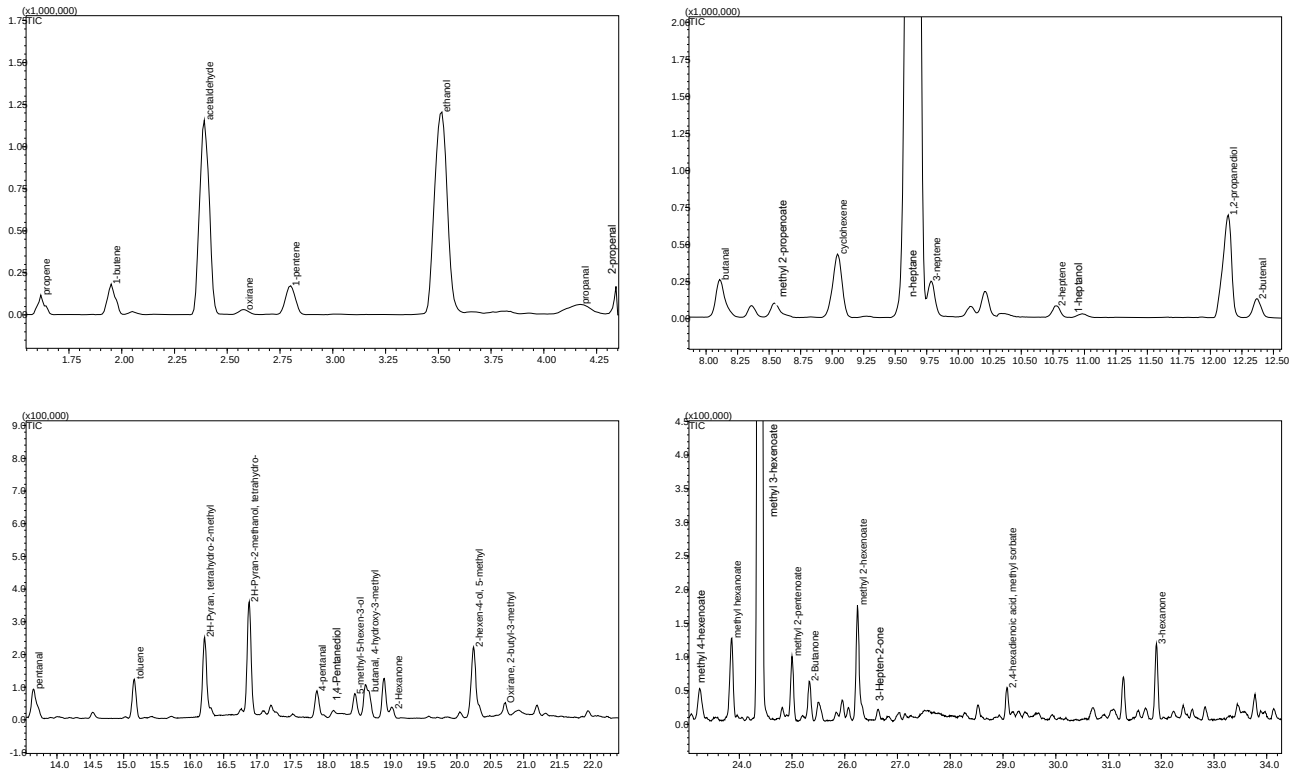

Appendix D: Product distribution in the oxidation of the mixture of ethanol, n-heptane, and methyl 3-hexenoate at compression ratio 5.3. Y-axis represents FID signal strength and X-axis is retention time. Samples were analyzed in HP-5890 GC with injection volume of 1 uL and a split ratio of 30.

Appendix E

Detailed Product Distribution of Low-Temperature Oxidation in the Mixture of Ethanol, n-Heptane, and Methyl Hexenoate e20/(mhx30/hept70)

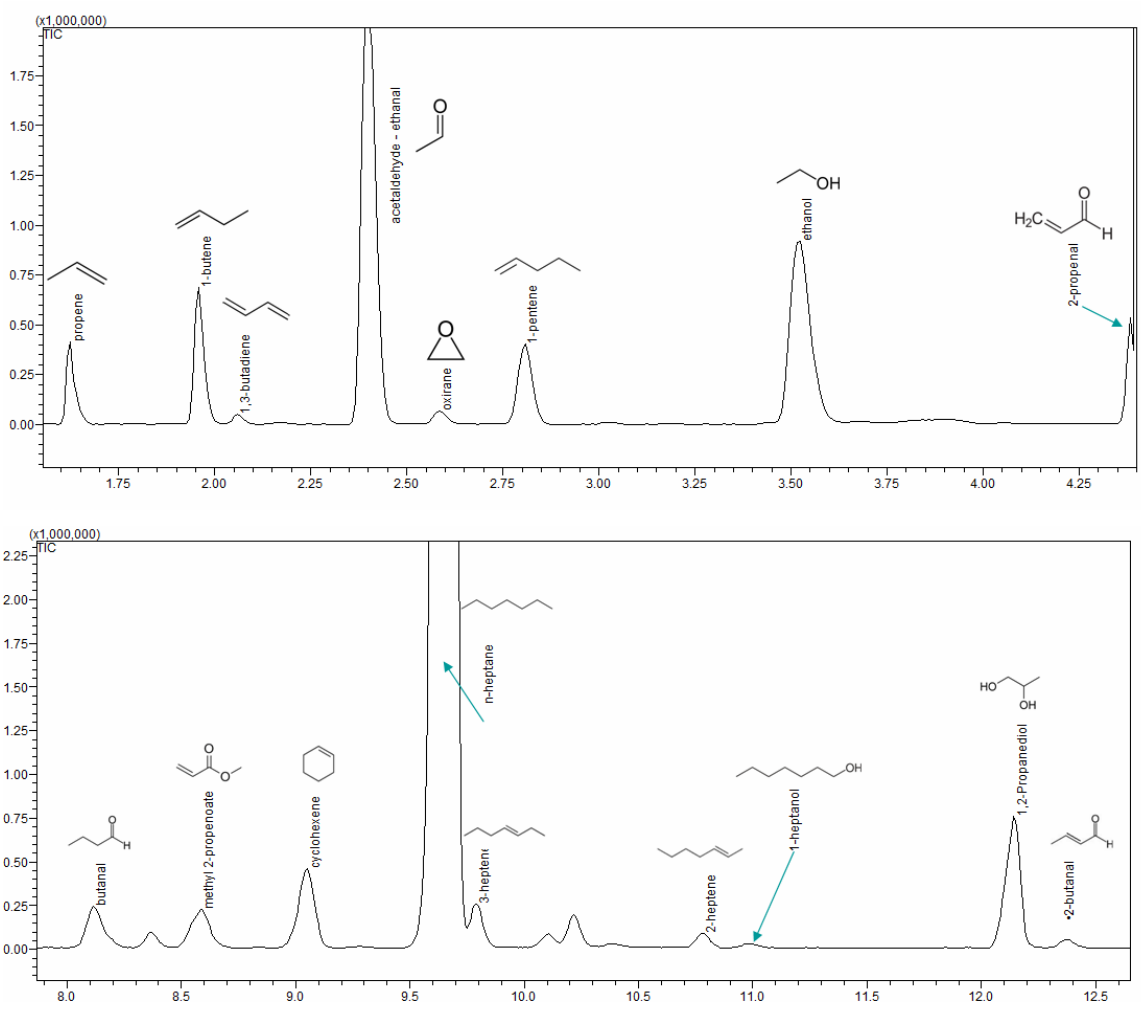

Appendix E: Detailed product distribution from appendix C: Retention time 1.5 - 12.5 minutes expanded

Appendix E

(continued)

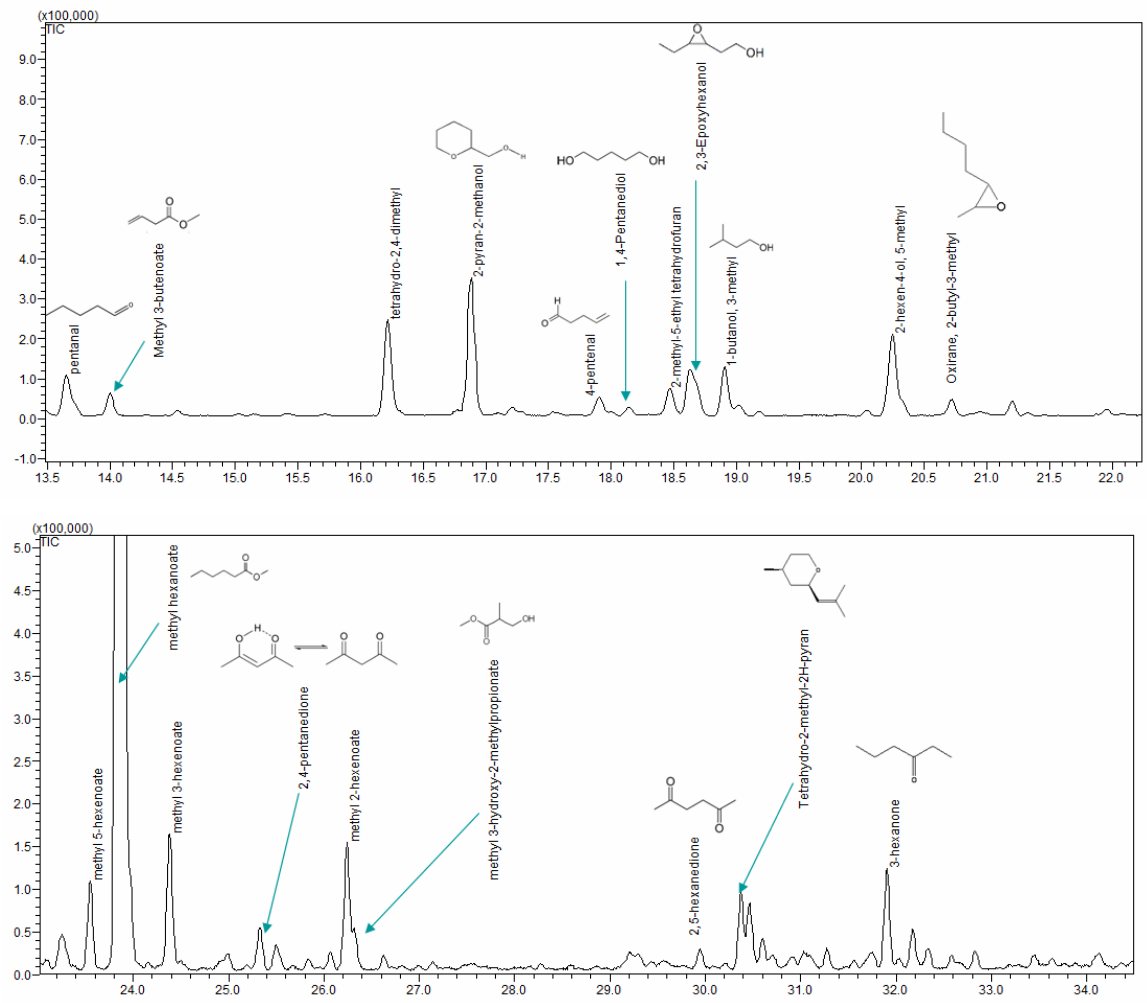

Appendix E (cont): Detailed product distribution from appendix C: Retention time 13.5 - 35 minutes expanded

Appendix F

Detailed Product Distribution of Low-Temperature Oxidation in the Mixture of Ethanol, n-Heptane, and Methyl 3-Hexenoate e20/(m3h30/hept70)

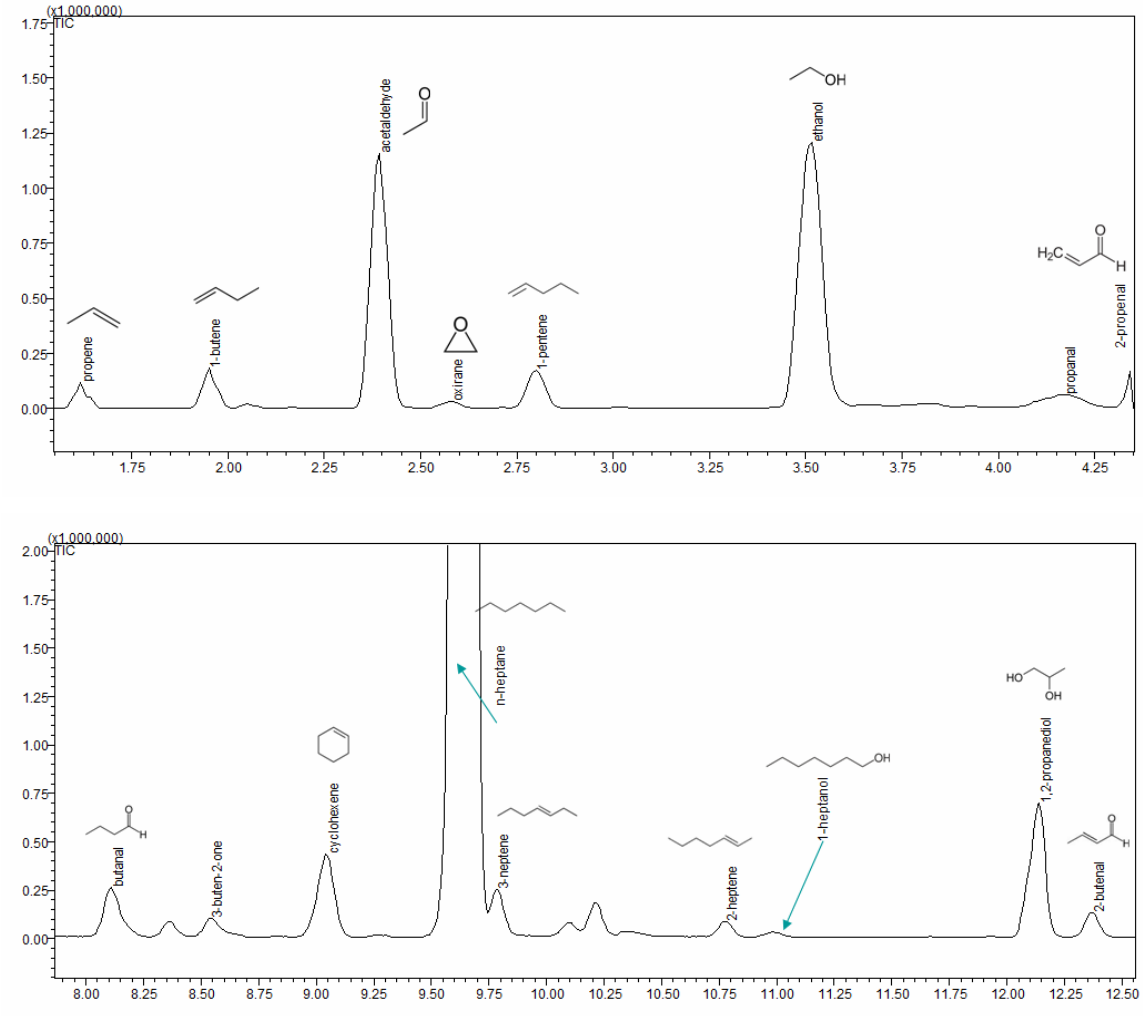

Appendix F: Detailed product distribution from appendix D: Retention time 1.5 - 12.5 minutes expanded

Appendix F
(continued)

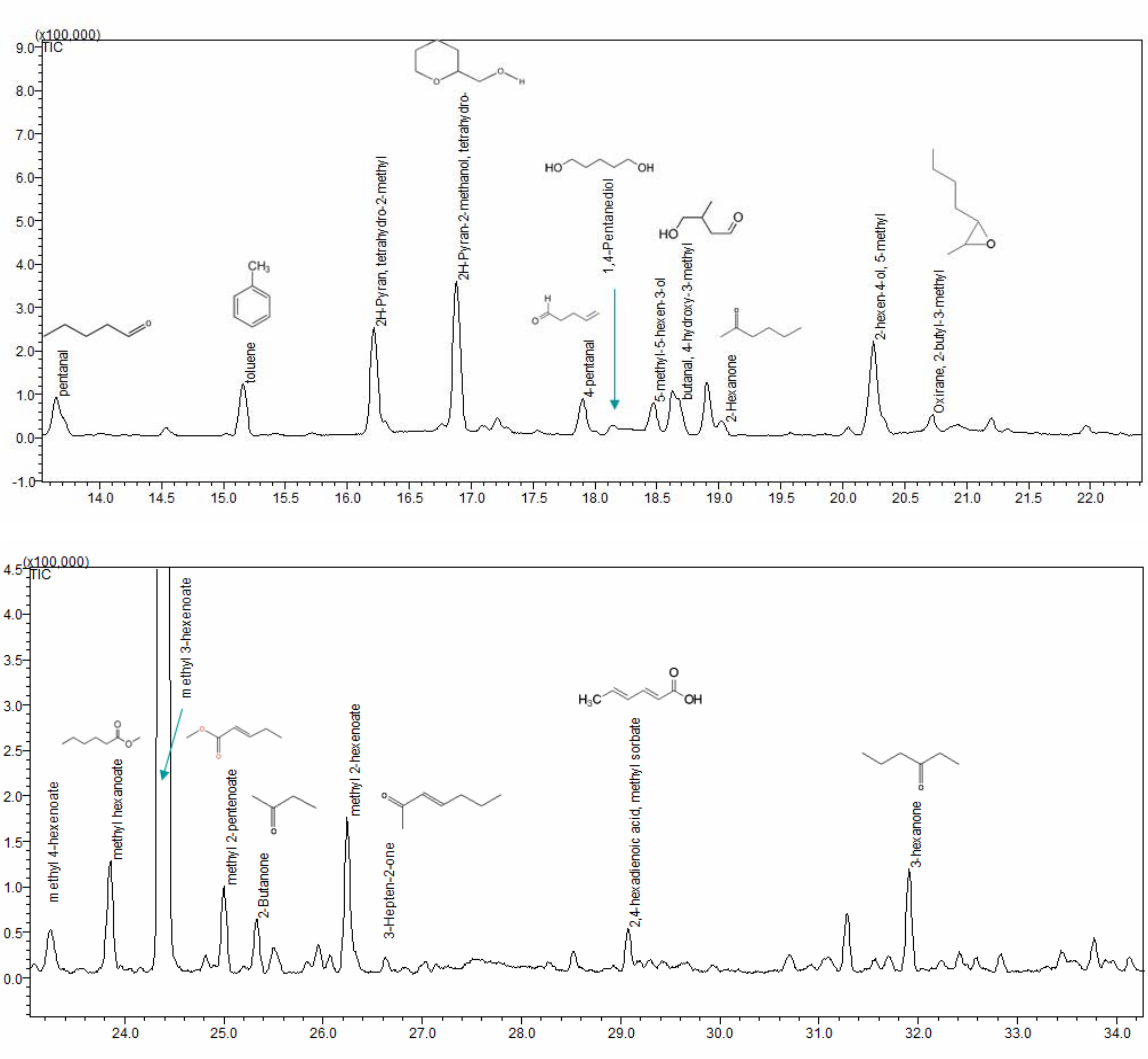

Appendix F (cont): Detailed product distribution from appendix D: Retention time 13.5 - 35 minutes expanded

Appendix G

Repeatability of Heat Release Results for n-Heptane at Φ=0.50

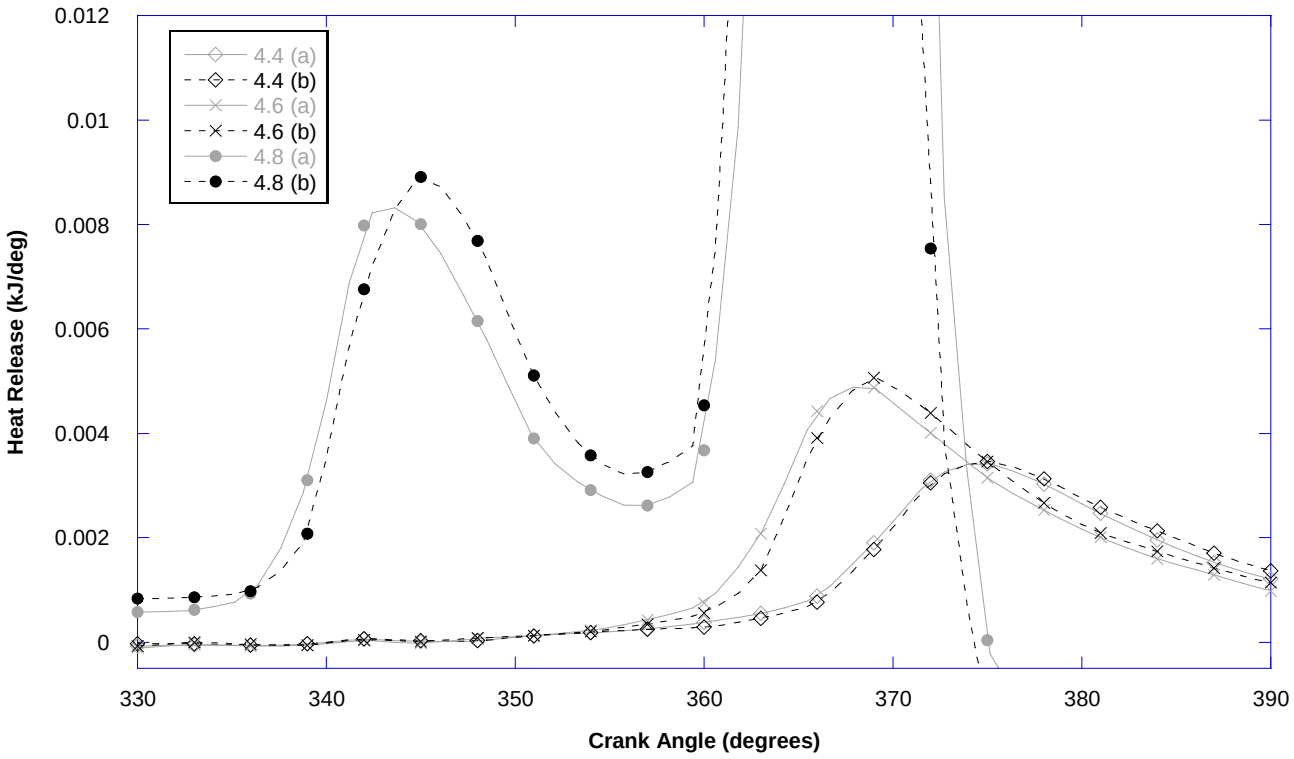

Appendix G: Heat release data from two separate runs for n-heptane at Φ=0.50 under the same conditions to demonstrate repeatability. Dashed black curves are test run #1 and solid grey curves are test run #2

Appendix H

Effect of a Fractional Increase in Equivalence Ratio for Methyl Hexanoate

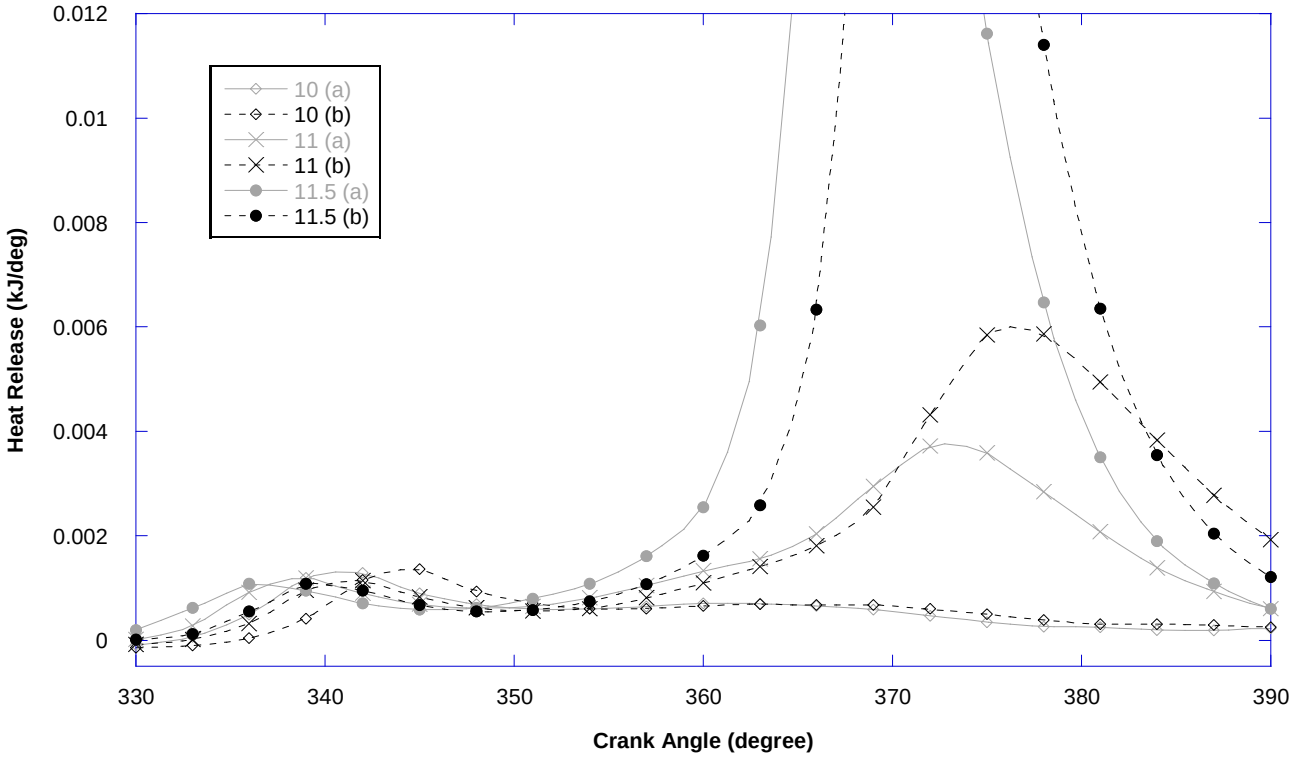

Appendix H: The effect of a marginal equivalence ratio increase from Φ=0.25 to Φ=0.29 on neat methyl hexanoate to demonstrate repeatability. Dashed black curves are Φ=0.29 and solid grey curves are Φ=0.25

Bibliography

1. Agarwal, A. K., Biofuels (alcohols and biodiesel) applications as fuels for internal combustion engines. *Progress in Energy and Combustion Science* **2007,** 33, (3), 233-271.

2. Lapuerta, M.; Armas, O.; Herreros, J. M., Emissions from a diesel-bioethanol blend in an automotive diesel engine. *Fuel* **2008,** 87, (1), 25-31.

3. Knothe, G., Biodiesel and renewable diesel: A comparison. *Progress in Energy and Combustion Science* **2010,** 36, (3), 364-373.

4. Hribernik, A.; Kegl, B., Influence of biodiesel fuel on the combustion and emission formation in a direct injection (DI) diesel engine. *Energy Fuels* **2007,** 21, (3), 1760-1767.

5. Hansen, A. C.; Zhang, Q.; Lyne, P. W. L., Ethanol-diesel fuel blends - a review. *Bioresource Technology* **2005,** 96, (3), 277-285.

6. Xue, J. L.; Grift, T. E.; Hansen, A. C., Effect of biodiesel on engine performances and emissions. *Renew. Sust. Energ. Rev.* **2011,** 15, (2), 1098-1116.

7. Tsolakis, A.; Megaritis, A.; Wyszynski, M. L.; Theinnoi, K., Engine performance and emissions of a diesel engine operating on diesel-RME (rapeseed methyl ester) blends with EGR (exhaust gas recirculation). *Energy* **2007,** 32, (11), 2072-2080.

8. Mueller, C.; Kilpinen, P.; Hupa, M., Influence of HCl on the homogeneous reactions of CO and NO in postcombustion conditions - A kinetic modeling study. *Combustion and Flame* **1998,** 113, (4), 579-588.

9. Tat, M. E.; Van Gerpen, J. H.; Soylu, S.; Canakci, M.; Monyem, A.; Wormley, S., The speed of sound and isentropic bulk modulus of biodiesel at 21 degrees C from atmospheric pressure to 35 MPa. *Journal of the American Oil Chemists Society* **2000,** 77, (3), 285-289.

10. Szybist, J.; Boehman, A., Behavior of a Diesel Injection System with Biodiesel Fuel. *Society of Automotive Engineers* **2003,** Technical Paper 2003-01-1039.

11. Ribeiro, N. M.; Pinto, A. C.; Quintella, C. M.; da Rocha, G. O.; Teixeira, L. S. G.; Guarieiro, L. L. N.; Rangel, M. D.; Veloso, M. C. C.; Rezende, M. J. C.; da Cruz, R. S.; de Oliveira, A. M.; Torres, E. A.; de Andrade, J. B., The role of additives for diesel and diesel blended (Ethanol or biodiesel) fuels: A review. *Energy Fuels* **2007,** 21, (4), 2433-2445.

12. Heywood, J. B., *Internal Combustion Engine Fundamentals. Chapter 11*. International Edition ed.; McGraw Hill Higher Education: 1989.

13. Westbrook, C. K., Chemical kinetics of hydrocarbon ignition in practical combustion systems. *Proceedings of the Combustion Institute* **2000,** 28, 1563-1577.

14. Rounce, P.; Tsolakis, A.; Leung, P.; York, A. P. E., A Comparison of Diesel and Biodiesel Emissions Using Dimethyl Carbonate as an Oxygenated Additive. *Energy Fuels* **2010,** 24, 4812-4819.

15. Chen, H.; Wang, J. X.; Shuai, S. J.; Chen, W. M., Study of oxygenated biomass fuel blends on a diesel engine. *Fuel* **2008,** 87, (15-16), 3462-3468.

16. Lapuerta, M.; Armas, O.; Garcia-Contreras, R., Stability of diesel-bioethanol blends for use in diesel engines. *Fuel* **2007,** 86, (10-11), 1351-1357.

17. Lapuerta, M.; Garcia-Contreras, R.; Campos-Fernandez, J.; Dorado, M. P., Stability, Lubricity, Viscosity, and Cold-Flow Properties of Alcohol-Diesel Blends. *Energy Fuels* **2010,** 24, 4497-4502.

18. Lapuerta, M.; Armas, O.; Garcia-Contreras, R., Effect of Ethanol on Blending Stability and Diesel Engine Emissions. *Energy Fuels* **2009,** 23, 4343-4354.

19. Torres-Jimenez, E.; Jerman, M. S.; Gregorc, A.; Lisec, I.; Dorado, M. P.; Kegl, B., Physical and chemical properties of ethanol-diesel fuel blends. *Fuel* **2011,** 90, (2), 795-802.

20. Lapuerta, M.; Garcia-Contreras, R.; Agudelo, J. R., Lubricity of Ethanol-Biodiesel-Diesel Fuel Blends. *Energy Fuels* **2010,** 24, 1374-1379.

21. Bannister, C. D.; Chuck, C. J.; Bounds, M.; Hawley, J. G., Oxidative stability of biodiesel fuel. *Proc. Inst. Mech. Eng. Part D-J. Automob. Eng.* **2011,** 225, (D1), 99-114.

22. HadjAli, K.; Crochet, M.; Vanhove, G.; Ribaucour, M.; Minetti, R., A study of the low temperature autoignition of methyl esters. *Proceedings of the Combustion Institute* **2009,** 32, 239-246.

23. Gail, S.; Thomson, M. J.; Sarathy, S. M.; Syed, S. A.; Dagaut, P.; Dievart, P.; Marchese, A. J.; Dryer, F. L., A wide-ranging kinetic modeling study of methyl butanoate combustion. *Proceedings of the Combustion Institute* **2007,** 31, 305-311.

24. Szybist, J. P.; Boehman, A. L.; Haworth, D. C.; Koga, H., Premixed ignition behavior of alternative diesel fuel-relevant compounds in a motored engine experiment. *Combustion and Flame* **2007,** 149, (1-2), 112-128.

25. Zhang, Y. Low Temperature Oxidation of Biodiesel Surrogates in a Motored Engine and the Oxidation Behavior of Soot Generated from the Combustion of a Biodiesel Surrogate in a Diffusion Flame. The Pennsylvania State University, 2010.

26. Ajav EA, S. B., Bhattacharya TK., Experimental study of some performance parameters of a constant speed stationary diesel engine using ethanol–diesel blends as fuel. In Biomass Bioenergy: 1999; pp 357–65.

27. Gary Borman, K. R., *Combustion Engineering*. McGraw-Hill Companies. Chapter 4: Nitrogen Oxide Kinetics: 1998; p 613.

28. Busca, G.; Lietti, L.; Ramis, G.; Berti, F., Chemical and mechanistic aspects of the selective catalytic reduction of NOx by ammonia over oxide catalysts: A review. *Appl. Catal. B-Environ.* **1998,** 18, (1-2), 1-36.

29. Ramadhas, A. S.; Jayaraj, S.; Muraleedharan, C., Use of vegetable oils as IC engine fuels - A review. *Renew. Energy* **2004,** 29, (5), 727-742.

30. Wu, F. J.; Wang, J. X.; Chen, W. M.; Shuai, S. J., A study on emission performance of a diesel engine fueled with five typical methyl ester biodiesels. *Atmospheric Environment* **2009,** 43, (7), 1481-1485.

31. Graboski MS, McCormick RL, Alleman TL, Herring AM. The effect of biodiesel composition on engine emissions from a DDC series 60 diesel engine. Natl Renew Energy Lab 2003. NREL/SR-510-31461. In.

32. Song, J. T.; Zhang, C. H., An experimental study on the performance and exhaust emissions of a diesel engine fuelled with soybean oil methyl ester. *Proceedings of the Institution of Mechanical Engineers Part D-Journal of Automobile Engineering* **2008,** 222, (D12), 2487-2496.

33. Kim, H.; Choi, B., The effect of biodiesel and bioethanol blended diesel fuel on nanoparticles and exhaust emissions from CRDI diesel engine. *Renewable Energy* **2010,** 35, (1), 157-163.

34. Cheung, C. S.; Zhu, L.; Huang, Z., Regulated and unregulated emissions from a diesel engine fueled with biodiesel and biodiesel blended with methanol. *Atmospheric Environment* **2009,** 43, (32), 4865-4872.

35. Johnson, T. V., Review of diesel emissions and control. *International Journal of Engine Research* **2009,** 10, (5), 275-285.

36. Rajasekar, E.; Murugesan, A.; Subramanian, R.; Nedunchezhian, N., Review of NOx reduction technologies in CI engines fuelled with oxygenated biomass fuels. *Renew. Sust. Energ. Rev.* **2010,** 14, (7), 2113-2121.

37. Zhang, Y.; Boehman, A. L., Oxidation of 1-butanol and a mixture of n-heptane/1-butanol in a motored engine. *Combust. Flame* **2010,** 157, (10), 1816-1824.

38. Brown, J. H. L. M. J. P. D. B., Evaluation of Cu-Based SCR/DPF Technology for Diesel Exhaust Emission Control. *International Journal of Engine Research* **2009,** Volume 10, (Number 5 / 2009).

39. Breen, J. P.; Burch, R., A review of the effect of the addition of hydrogen in the selective catalytic reduction of NOx with hydrocarbons on silver catalysts. *Top. Catal.* **2006,** 39, (1-2), 53-58.

40. Satokawa, S.; Shibata, J.; Shimizu, K.; Atsushi, S.; Hattori, T., Promotion effect of H-2 on the low temperature activity of the selective reduction of NO by light hydrocarbons over Ag/Al2O3. *Appl. Catal. B-Environ.* **2003,** 42, (2), 179-186.

41. Seong, H. J.; Boehman, A. L., Impact of Intake Oxygen Enrichment on Oxidative Reactivity and Properties of Diesel Soot. *Energy Fuels* **2011,** 25, 602-616.

42. Song, J. H.; Alam, M.; Boehman, A. L.; Kim, U., Examination of the oxidation behavior of biodiesel soot. *Combust. Flame* **2006,** 146, (4), 589-604.

43. Al-Qurashi, K.; Boehman, A. L., Impact of exhaust gas recirculation (EGR) on the oxidative reactivity of diesel engine soot. *Combust. Flame* **2008,** 155, (4), 675-695.

44. Vander Wal, R. L., Initial investigation of effects of fuel oxygenation on nanostructure of soot from a direct-injection diesel engine. *Energy Fuels* **2006,** 20, (6), 2364-2369.

45. Muller, J. O.; Su, D. S.; Jentoft, R. E.; Krohnert, J.; Jentoft, F. C.; Schlogl, R., Morphology-controlled reactivity of carbonaceous materials towards oxidation. *Catal. Today* **2005,** 102, 259-265.

46. Curran, H. J.; Gaffuri, P.; Pitz, W. J.; Westbrook, C. K., A comprehensive modeling study of n-heptane oxidation. *Combustion and Flame* **1998,** 114, (1-2), 149-177.

47. Glassman, I.; Yetter, R. A.; ScienceDirect (Online service), Combustion. In 4th ed.; Academic Press: Amsterdam ; Boston, 2008; pp xx, 773 p.

48. Dagaut, P.; Reuillon, M.; Cathonnet, M., Experimental-Study Of The Oxidation Of N-Heptane In A Jet-Stirred Reactor From Low-Temperature To High-Temperature And Pressures Up To 40-Atm. *Combustion And Flame* **1995,** 101, (1-2), 132-140.

49. Gaffuri, P.; Faravelli, T.; Ranzi, E.; Cernansky, N. P.; Miller, D.; dAnna, A.; Ciajolo, A., Comprehensive kinetic model for the low-temperature oxidation of hydrocarbons. *Aiche Journal* **1997,** 43, (5), 1278-1286.

50. Dayma, G.; Gail, S.; Dagaut, P., Experimental and kinetic modeling study of the oxidation of methyl hexanoate. *Energy & Fuels* **2008,** 22, (3), 1469-1479.

51. Glaude, P. A.; Herbinet, O.; Bax, S.; Biet, J.; Warth, V.; Battin-Leclerc, F., Modeling of the oxidation of methyl esters-Validation for methyl hexanoate, methyl heptanoate, and methyl decanoate in a jet-stirred reactor. *Combustion and Flame* **2010,** 157, (11), 2035-2050.

52. Zhang, Y.; Boehman, A. L., Low temperature oxidation of methyl hexanoate in a motored engine. *Abstracts of Papers of the American Chemical Society* **2009,** 238, 172-FUEL.

53. Leppard, W. R., *A Comparison of Olefin and Paraffin Autoignition Chemistries: A Motored Engine Study*. *SAE 892081* **1989**.

54. Tanaka, S.; Ayala, F.; Keck, J. C.; Heywood, J. B., Two-stage ignition in HCCI combustion and HCCI control by fuels and additives. *Combustion and Flame* **2003,** 132, (1-2), 219-239.